



Computational methods for the dynamics of the nonlinear Schrödinger/Gross-Pitaevskii equations

Xavier Antoine^{a,b}, Weizhu Bao^{1c,d}, Christophe Besse^e

^aUniversité de Lorraine, Institut Elie Cartan de Lorraine, UMR 7502, Vandoeuvre-lès-Nancy, F-54506, France

^bCNRS, Institut Elie Cartan de Lorraine, UMR 7502, Vandoeuvre-lès-Nancy, F-54506, France

^cDepartment of Mathematics, National University of Singapore, Singapore 119076, Singapore

^dCenter for Computational Science and Engineering, National University of Singapore, Singapore 119076, Singapore

^eLaboratoire Paul Painlevé, Université Lille Nord de France, CNRS UMR 8524, INRIA SIMPAF Team, Université Lille 1 Sciences et Technologies, Cité Scientifique, 59655 Villeneuve d'Ascq Cedex, France

Abstract

In this paper, we begin with the nonlinear Schrödinger/Gross-Pitaevskii equation (NLSE/GPE) for modeling Bose-Einstein condensation (BEC) and nonlinear optics as well as other applications, and discuss their dynamical properties ranging from time reversible, time transverse invariant, mass and energy conservation, dispersion relation to soliton solutions. Then, we review and compare different numerical methods for solving the NLSE/GPE including finite difference time domain methods and time-splitting spectral method, and discuss different absorbing boundary conditions. In addition, these numerical methods are extended to the NLSE/GPE with damping terms and/or an angular momentum rotation term as well as coupled NLSEs/GPEs. Finally, applications to simulate a quantized vortex lattice dynamics in a rotating BEC are reported.

© 2011 Published by Elsevier Ltd.

Keywords: nonlinear Schrödinger equation, Gross-Pitaevskii equation, time-splitting spectral method, Crank-Nicolson finite difference method, absorbing boundary condition, Bose-Einstein condensation

PACS: 02.60.-x, 02.70.-c, 31.15.-p, 31.15.xf

2010 MSC: 35Q41, 65M06, 65M12, 65M70, 65Z05, 78M20, 78M22, 81Q05, 81Q20, 81V45

1. Introduction

The nonlinear Schrödinger equation (NLSE) is a partial differential equation (PDE) that can be met in many different areas of physics and chemistry as well as engineering [1, 2, 84, 92, 158, 165, 170]. The most well-known and important derivation of the NLSE is from the mean-field approximation of many-body problems in quantum physics and chemistry [158], especially for the study of Bose-Einstein condensation (BEC) [11, 158], where it is also called the Gross-Pitaevskii equation (GPE) [29, 118, 157, 158]. Another important application of the NLSE is for laser beam propagation in nonlinear and/or quantum optics and there it is also known as parabolic/paraxial approximation of the Helmholtz or time-independent Maxwell equations [1, 2, 84, 170]. Other important applications include long

¹Corresponding author

Email addresses: xavier.antoine@univ-lorraine.fr (Xavier Antoine), bao@math.nus.edu.sg (Weizhu Bao), christophe.besse@math.univ-lille1.fr (Christophe Besse)

URL: <http://www.math.nus.edu.sg/~bao/> (Weizhu Bao)

range wave propagation in underwater acoustics [152, 170], plasma and particle physics [170], semiconductor industry [143, 146], materials simulation based on the first principle [101], superfluids [5, 57], molecular systems in biology [85].

In this paper, we consider the following time-dependent NLSE [29, 170]

$$i\varepsilon\partial_t\psi(t, \mathbf{x}) = -\frac{\varepsilon^2}{2}\nabla^2\psi(t, \mathbf{x}) + V(\mathbf{x})\psi(t, \mathbf{x}) + f(|\psi(t, \mathbf{x})|^2)\psi(t, \mathbf{x}), \quad \mathbf{x} \in \mathbb{R}^d, \quad t > 0, \quad (1.1)$$

with initial data

$$\psi(t = 0, \mathbf{x}) = \psi_0(\mathbf{x}), \quad \mathbf{x} \in \mathbb{R}^d, \quad (1.2)$$

where $i = \sqrt{-1}$ is the complex unit, t is the time variable, $\mathbf{x} \in \mathbb{R}^d$ is the spatial variable with $d = 1, 2, 3$, $\psi := \psi(t, \mathbf{x})$ is the complex-valued wave function or order parameter, $\nabla^2 = \Delta$ is the usual Laplace operator and $\psi_0 := \psi_0(\mathbf{x})$ is a given complex-valued initial data. Moreover, $0 < \varepsilon \leq 1$ is a dimensionless parameter. In most physics literatures, it is taken equal to $\varepsilon = 1$; however in the semi-classical regime, we have $0 < \varepsilon \ll 1$, ε being also called the "scaled" Planck constant. Function $V := V(\mathbf{x})$ is a given real-valued external potential and its specific form depends on different applications and could also sometimes be time dependent [27, 29, 158, 170]. For example, in BEC, it is usually chosen as either a harmonic confining potential, i.e. $V(\mathbf{x}) = \frac{|\mathbf{x}|^2}{2}$ [27, 29, 158] or an optical lattice potential, i.e. $V(\mathbf{x}) = A_1 \cos(L_1 x) + A_2 \cos(L_2 y) + A_3 \cos(L_3 z)$ in three dimensions (3D) with A_1, A_2, A_3, L_1, L_2 and L_3 constants [27, 29, 124, 125, 158], or a stochastic potential for producing speckle patterns [148, 158]; in nonlinear optics, it might be chosen as an attractive potential, i.e. $V(\mathbf{x}) = -\frac{|\mathbf{x}|^2}{2}$ [1, 84]. The nonlinearity $f := f(\rho)$ is a real-valued smooth function depending on the density $\rho := |\psi|^2 \in [0, \infty)$ and its specific form depends on different applications [1, 2, 27, 29, 158, 170]. In fact, when $f(\rho) \equiv \lambda$, with λ a constant, then the NLSE (1.1) collapses to the standard (linear) Schrödinger equation [92, 165]. The most popular and important nonlinearity is the cubic nonlinearity [1, 2, 29, 158, 170]

$$f(\rho) = \beta\rho, \quad 0 \leq \rho < \infty, \quad (1.3)$$

where β (positive for repulsive or defocusing interaction and negative for attractive or focusing interaction) is a given dimensionless constant describing the strength of interaction. Other nonlinearities used in nonlinear optics include the cubic-quintic nonlinearity $f(\rho) = \beta_1\rho + \beta_2\rho^2$ [1, 84, 152, 170] and the saturation of the intensity nonlinearity $f(\rho) = \frac{\beta_0\rho}{1+c_0\rho}$ with $\beta_0, \beta_1, \beta_2$ and c_0 given constants [1, 84, 152, 170]. In some applications, nonlocal nonlinearities can also be considered, and in this case $f(\rho) = U * \rho$ which is a convolution, with $U := U(\mathbf{x})$ the kernel [29, 33, 44, 56, 65, 185]. Specifically, for the Hartree potential case, $U(\mathbf{x}) = \frac{1}{4\pi|\mathbf{x}|}$ is the Green's function of the Laplace operator in 3D, and then, the NLSE (1.1) can be re-written as the Schrödinger-Poisson system in 3D [56, 38]. Finally, we remark here that the NLSE (1.1) is also called the Gross-Pitaevskii Equation (GPE) when the nonlinearity is chosen as the cubic nonlinearity as in (1.3), especially in BEC [27, 29, 158]. Thus GPE is a special version of NLSE [27, 29, 118, 157, 158].

There are many important dynamical properties of the solution ψ to the NLSE (1.1). Among them, here we mention several important ones that we will use to justify different numerical methods on whether they are still valid at the discrete level after the NLSE (1.1) is discretized by a numerical method. In fact, the NLSE (1.1) is a dispersive PDE and it is *time reversible or symmetric*, i.e. it is unchanged under the change of variable in time as $t \rightarrow -t$ and taken conjugate in the equation. Another important property is *time transverse or gauge invariant*, i.e. if $V \rightarrow V + \alpha$, with α a given real constant, then the solution $\psi \rightarrow \psi e^{-i\alpha t/\varepsilon}$ which immediately implies that the density $\rho = |\psi|^2$ is unchanged. The NLSE (1.1) conserves many quantities. Among them, the *mass* (or wave energy in nonlinear optics) and *energy* (or Hamiltonian in nonlinear optics) *conservation* are given as [29, 74, 170]

$$N(t) := \|\psi(t, \cdot)\|^2 = \int_{\mathbb{R}^d} |\psi(t, \mathbf{x})|^2 d\mathbf{x} \equiv \int_{\mathbb{R}^d} |\psi(0, \mathbf{x})|^2 d\mathbf{x} = \int_{\mathbb{R}^d} |\psi_0(\mathbf{x})|^2 d\mathbf{x} := N(0), \quad t \geq 0, \quad (1.4)$$

$$E(t) := \int_{\mathbb{R}^d} \left[\frac{\varepsilon^2}{2} |\nabla\psi(t, \mathbf{x})|^2 + V(\mathbf{x})|\psi(t, \mathbf{x})|^2 + F(|\psi(t, \mathbf{x})|^2) \right] d\mathbf{x} \equiv E(0), \quad t \geq 0, \quad (1.5)$$

respectively, with

$$F(\rho) := \int_0^\rho f(s) ds, \quad 0 \leq \rho < +\infty. \quad (1.6)$$

If there is no external potential in the NLSE (1.1), i.e. $V(\mathbf{x}) \equiv 0$, then the momentum and angular momentum are also conserved [29, 74, 170]. In addition, the NLSE (1.1) admits the plane wave solution as $\psi(t, \mathbf{x}) = Ae^{i(\mathbf{k}\cdot\mathbf{x}-\omega t)}$, where the time frequency ω , amplitude A and spatial wave number \mathbf{k} satisfy the following *dispersion relation* [29, 74, 126, 170]

$$\omega = \frac{\varepsilon|\mathbf{k}|^2}{2} + \frac{1}{\varepsilon}f(|A|^2). \quad (1.7)$$

In this case, if in 1D with $\varepsilon = 1$ and the nonlinearity is chosen as the focusing cubic nonlinearity (1.3) with $\beta < 0$, it also admits the well-known bright soliton solution as [1, 2, 49, 84, 152, 170]

$$\psi_B(t, x) = \frac{A}{\sqrt{-\beta}} \operatorname{sech}(A(x - vt - x_0)) e^{i(vx - \frac{1}{2}(v^2 - A^2)t + \theta_0)}, \quad x \in \mathbb{R}, \quad t \geq 0, \quad (1.8)$$

where $\frac{A}{\sqrt{-\beta}}$ is the amplitude of the soliton with A a real constant, v is the velocity of the soliton, x_0 and θ_0 are the initial shifts in space and phase, respectively. Since the soliton solution is exponentially decaying for $|x| \rightarrow +\infty$, then the mass and energy are well defined and given by: $N(\psi_B) = -\frac{2A}{\beta}$ and $E(\psi_B) = \frac{Av^2}{-\beta} + \frac{A^3}{-3\beta}$. For other more dynamical properties of the NLSE (1.1) such as dark (black and grey) solitons in 1D under defocusing cubic nonlinearity, well-posedness and finite time blow-up, we refer to [29, 74, 108, 109, 170] and references therein.

For studying numerically the dynamics of the NLSE (1.1), different numerical methods have been proposed in the literatures [9, 12, 27, 29, 36, 39, 40, 61, 78, 77, 75, 76, 99, 119, 120, 130, 144, 156, 173, 182] and references therein. The main aim of this paper is to review different numerical methods for solving the NLSE (1.1) numerically, compare them in terms of keeping different dynamical properties at the discretized level, stability and accuracy, discuss different absorbing boundary conditions for truncating the NLSE (1.1) onto a bounded computational domain, and extend them for solving NLSE with damping and/or angular momentum terms as well as coupled NLSEs.

The paper is organized as follows. In Section 2, we review several popular numerical methods in the literatures for discretizing NLSE/GPE under simple boundary conditions and compare their advantages and disadvantages, discuss different absorbing boundary conditions for NLSE/GPE, and review some robust and efficient numerical methods for NLSE/GPE in the semiclassical regime. Extensions to NLSE/GPE with damping and/or angular rotating terms and coupled NLSEs/GPEs are presented in Sections 3 and 4, respectively. Numerical comparison of different numerical methods and some applications are reported in Section 5. Finally, we draw some conclusions and discuss future perspectives in Section 6.

2. Numerical methods for NLSE/GPE

2.1. Some popular numerical methods

Here we present several popular numerical methods for discretizing the NLSE/GPE (1.1) and discuss/compare their properties including stability, accuracy, computational cost and how much properties of NLSE/GPE that these numerical methods can keep at the discretized level. For simplicity of notation, we shall introduce these methods in one space dimension (1D), i.e. $d = 1$ in (1.1). Generalizations to $d > 1$ are straightforward for tensor product grids and the results remain valid with modifications. For $d = 1$, the NLSE/GPE (1.1) truncated on a bounded interval (a, b) with homogeneous Dirichlet boundary condition ($|a|$ and b large enough so that the error due to the truncation is negligible) becomes

$$i\varepsilon\partial_t\psi(t, x) = -\frac{\varepsilon^2}{2}\partial_{xx}\psi(t, x) + V(x)\psi(t, x) + f(|\psi(t, x)|^2)\psi(t, x), \quad a < x < b, \quad t > 0, \quad (2.1)$$

$$\psi(t, a) = \psi(t, b) = 0, \quad t \geq 0, \quad (2.2)$$

$$\psi(t = 0, x) = \psi_0(x), \quad a \leq x \leq b. \quad (2.3)$$

In this case, the *mass and energy conservation* collapse to the following

$$N(t) := \|\psi(t, \cdot)\|^2 = \int_a^b |\psi(t, x)|^2 dx \equiv \int_a^b |\psi(0, x)|^2 dx = \int_a^b |\psi_0(x)|^2 dx := N(0), \quad t \geq 0, \quad (2.4)$$

$$E(t) := \int_a^b \left[\frac{\varepsilon^2}{2} |\partial_x \psi(t, x)|^2 + V(x) |\psi(t, x)|^2 + F(|\psi(t, x)|^2) \right] dx \equiv E(0), \quad t \geq 0. \quad (2.5)$$

Choose a time step $\tau := \Delta t > 0$ and denote the different times as $t_n := n\tau$ for $n = 0, 1, 2, \dots$; choose the mesh size $h := \Delta x = \frac{b-a}{J}$, with J an even positive integer, and denote the grid points by $x_j := a + jh$, for $j = 0, 1, \dots, J$. Let ψ_j^n be the numerical approximation of $\psi(t_n, x_j)$, for $j = 0, 1, \dots, J$ and $n = 0, 1, 2, \dots$; let Ψ^n be the solution vector at time $t = t_n$ with components $(\psi_j^n)_{0 \leq j \leq J}$. In addition, for any complex-valued vector $\phi = (\phi_j)_{0 \leq j \leq J}$, we define the following finite difference operators

$$(D_x^+ \phi)_j = \frac{\phi_{j+1} - \phi_j}{h}, \quad 0 \leq j \leq J-1; \quad (D_x^2 \phi)_j = \frac{\phi_{j+1} - 2\phi_j + \phi_{j-1}}{h^2}, \quad 1 \leq j \leq J-1. \quad (2.6)$$

Then the *Crank-Nicolson finite difference* (CNFD) method — in which one applies the second-order centered difference scheme for spatial discretization and the Crank-Nicolson scheme for time discretization — for discretizing (2.1) reads as [29, 30, 80, 79, 115, 119, 196]

$$i\varepsilon \frac{\psi_j^{n+1} - \psi_j^n}{\tau} = -\frac{\varepsilon^2}{4} \left[(D_x^2 \Psi^{n+1})_j + (D_x^2 \Psi^n)_j \right] + \left[V(x_j) + G(|\psi_j^{n+1}|^2, |\psi_j^n|^2) \right] \frac{\psi_j^{n+1} + \psi_j^n}{2}, \quad 1 \leq j \leq J-1, \quad n \geq 0, \quad (2.7)$$

where

$$G(\rho_1, \rho_2) = \frac{F(\rho_1) - F(\rho_2)}{\rho_1 - \rho_2} := \int_0^1 f(\theta\rho_1 + (1-\theta)\rho_2) d\theta, \quad 0 \leq \rho_1, \rho_2 < \infty.$$

The boundary and initial conditions (2.2)-(2.3) are discretized as

$$\psi_0^{n+1} = \psi_J^{n+1} = 0, \quad n \geq 0; \quad \psi_j^0 = \psi_0(x_j), \quad 0 \leq j \leq J. \quad (2.8)$$

The above CNFD method (2.7) is *time reversible or symmetric*, i.e. it is unchanged if $\tau \rightarrow -\tau$ and $n+1 \leftrightarrow n$; and its memory cost is $O(J^d)$ in d -dimensions with J unknowns in each direction. It conserves the *mass* (2.4) and *energy* (2.5) in the discretized level [29, 30, 31, 79, 115], i.e.

$$N^n := h \sum_{j=1}^{J-1} |\psi_j^n|^2 \equiv h \sum_{j=1}^{J-1} |\psi_j^0|^2 = h \sum_{j=1}^{J-1} |\psi_0(x_j)|^2 := N^0, \quad n \geq 0, \quad (2.9)$$

$$E^n := h \sum_{j=0}^{J-1} \left[\frac{\varepsilon^2}{2} |(D_x^+ \Psi^n)_j|^2 + V(x_j) |\psi_j^n|^2 + F(|\psi_j^n|^2) \right] \equiv E^0, \quad n \geq 0, \quad (2.10)$$

which immediately implies that the CNFD method is unconditionally stable. In addition, it can be proven rigorously in mathematics that the CNFD method is second-order accurate in both time and space for any fixed $\varepsilon = \varepsilon_0 = O(1)$ [29, 30, 31, 79, 115]. However, it cannot preserve the *time transverse invariant* and *dispersion relation* properties of the NLSE/GPE (2.1) at the discretized level [29, 30, 31]. Furthermore, it is an implicit scheme and its practical implementation is a little tedious. In fact, at each time step, one needs to solve a coupled fully nonlinear system which can be solved by a fixed point or a modified Newton-Raphson iterative method [7, 8, 9, 29, 30, 31] and thus it might be very time consuming. In general, the computational cost per time step is much larger than $O(J^d)$, especially in 2D and 3D. In fact, if the nonlinear system in (2.7) is not solved very accurately, e.g. up to machine precision, the numerical solution computed from (2.7) does not conserve the energy in (2.10) *exactly* [31].

Due to the high computational cost of the CNFD method, in the literatures it is motivated for considering some semi-implicit methods in which a linear system is to be solved at every time step. Thus, the computational cost is significantly reduced, especially in 2D and 3D. One of these numerical methods is the *relaxation finite difference* (ReFD) method — in which one gives a name to the nonlinear term and makes a second-order approximation at time t_n — for the NLSE (2.1) [61]

$$\begin{cases} \frac{1}{2} (u_j^{n+1/2} + u_j^{n-1/2}) = f(|\psi_j^n|^2), & 1 \leq j \leq J-1, \quad n \geq 0, \\ i\varepsilon \frac{\psi_j^{n+1} - \psi_j^n}{\tau} = -\frac{\varepsilon^2}{4} \left[(D_x^2 \Psi^{n+1})_j + (D_x^2 \Psi^n)_j \right] + \frac{1}{2} \left[V(x_j) + u_j^{n+1/2} \right] (\psi_j^{n+1} + \psi_j^n), \end{cases} \quad (2.11)$$

where $u_j^{-1/2} = \psi_j^0 = \psi_0(x_j)$ for $0 \leq j \leq J$. The boundary and initial conditions (2.2)-(2.3) are discretized as (2.8). Similarly, this ReFD method is *time reversible or symmetric*, its memory cost is $O(J^d)$ in d -dimensions with J

unknowns in each direction, and it is easier to be implemented than that of CNFD. It is an implicit scheme where, at each time step, only a linear system needs to be solved for example by the Thomas algorithm at the cost of $O(J)$ in 1D and by some iterative methods such as conjugate gradient (CG) or multigrid (MG) method [61, 81] in 2D and 3D at the cost, in general, larger than $O(J^d)$. Thus it is computationally much cheaper than that of the CNFD method. It conserves the mass (1.4) at the discretized level as (2.9) [61], and thus it is unconditionally stable. In addition, it can be mathematically proven rigorously that the ReFD method is second-order accurate in both time and space for any fixed $\varepsilon = \varepsilon_0 = O(1)$ [61]. Furthermore, for the NLSE with the cubic nonlinearity (1.3), this method also conserves the following discrete energy defined as

$$\tilde{E}^n := h \sum_{j=0}^{J-1} \frac{\varepsilon^2}{2} |(D_x^+ \psi^n)_j|^2 + h \sum_{j=1}^{J-1} \left[V(x_j) |\psi_j^n|^2 + \frac{\beta}{2} u_j^{n+1/2} u_j^{n-1/2} \right] \equiv \tilde{E}^0, \quad n \geq 0. \quad (2.12)$$

Of course, it cannot preserve the *time transverse invariant* and *dispersion relation* properties of the NLSE/GPE (2.1) in the discretized level [61]. In addition, for general nonlinearity other than the cubic nonlinearity, no discrete energy conservation has been proven for the ReFD method yet. Another popular method is the following *semi-implicit finite difference* (SIFD) method — in which one uses the leap-frog scheme for the nonlinear term in time discretization — for the NLSE (2.1) [30, 29, 31]

$$i\varepsilon \frac{\psi_j^{n+1} - \psi_j^{n-1}}{2\tau} = -\frac{\varepsilon^2}{4} \left[(D_x^2 \psi^{n+1})_j + (D_x^2 \psi^{n-1})_j \right] + [V(x_j) + f(|\psi_j^n|^2)] \psi_j^n, \quad 1 \leq j \leq J-1, \quad n \geq 1; \quad (2.13)$$

or

$$i\varepsilon \frac{\psi_j^{n+1} - \psi_j^{n-1}}{2\tau} = -\frac{\varepsilon^2}{4} \left[(D_x^2 \psi^{n+1})_j + (D_x^2 \psi^{n-1})_j \right] + V(x_j) \frac{\psi_j^{n+1} + \psi_j^{n-1}}{2} + f(|\psi_j^n|^2) \psi_j^n, \quad 1 \leq j \leq J-1, \quad n \geq 1; \quad (2.14)$$

The boundary and initial conditions (2.2)-(2.3) are discretized as (2.8) and the first step can be computed as [29, 30, 31]

$$\psi_j^1 = \psi_j^0 - \frac{i\tau}{\varepsilon} \left[-\frac{\varepsilon^2}{2} (D_x^2 \psi^0)_j + V(x_j) \psi_j^0 + f(|\psi_j^0|^2) \psi_j^0 \right], \quad 1 \leq j \leq J-1. \quad (2.15)$$

Again, this SIFD method is *time reversible* or *symmetric*, i.e. it is unchanged if $\tau \rightarrow -\tau$ and $n+1 \leftrightarrow n-1$; its memory cost is $O(J^d)$ in d -dimensions considering J unknowns in each direction. It is also much easier to be implemented than that of CNFD and ReFD, especially in 2D and 3D. It is an implicit scheme where, at each time step, only a linear system (whose coefficient matrix is time independent) needs to be solved, by the Thomas algorithm in $O(J)$ operations in 1D and by the direct fast Poisson solver *via* the discrete sine transform (DST) at the cost of $O(J^d \ln J)$ in 2D and 3D. Thus, it is significantly cheaper than the CNFD and ReFD methods, especially in 2D/3D. In addition, it can be proven that the SIFD method is second-order accurate both in time and space for any fixed $\varepsilon = \varepsilon_0 = O(1)$ [29, 30, 31] and a fourth-order (or six-order or even eighth-order) accurate method can be very easily constructed *via* the Richardson extrapolation technique [181]. Of course, it is conditionally stable under the stability condition $\tau \lesssim \tau_n := \frac{1}{\varepsilon \max_{0 \leq j \leq J} |V(x_j) + f(|\psi_j^n|^2)|}$ (or $\tau \lesssim \tau_n := \frac{1}{\varepsilon \max_{0 \leq j \leq J} |f(|\psi_j^n|^2)|}$ for (2.14)) for $n \geq 0$, which is independent of the mesh size h . It cannot preserve the *time transverse invariant*, *dispersion relation* and *mass and energy conservation* properties of the NLSE/GPE (2.1) in the discretized level [29, 30, 31].

Another way to handle the nonlinearity in (2.1) is to use the time-splitting technique [29, 36, 39, 40, 45, 124, 125, 66, 120, 156, 173, 174, 182], i.e. from time $t = t_n$ to time $t = t_{n+1}$, the equation (2.1) is solved in two splitting steps. One solves first

$$i\varepsilon \partial_t \psi(t, x) = -\frac{\varepsilon^2}{2} \partial_{xx} \psi(t, x), \quad a < x < b, \quad t > t_n, \quad (2.16)$$

with the homogeneous Dirichlet boundary condition (2.2) for the time step of length τ , followed by solving

$$i\varepsilon \partial_t \psi(t, x) = V(x) \psi(t, x) + f(|\psi(t, x)|^2) \psi(t, x), \quad a \leq x \leq b, \quad t > t_n, \quad (2.17)$$

for the same time step. Eq. (2.16) will be first discretized in space by the sine spectral method and then integrated (in phase space) in time *exactly* [29, 36, 39, 40, 53]. Multiplying (2.17) by $\overline{\psi(t, \mathbf{x})}$ (conjugate of $\psi(t, \mathbf{x})$) and then subtracting from its conjugate [29, 36, 39, 40], we get for $\rho(t, x) := |\psi(t, x)|^2$

$$\partial_t \rho(t, x) = 0, \quad t > t_n, \quad a \leq x \leq b, \quad (2.18)$$

which immediately implies that the density ρ is invariant for any fixed x in the second splitting step (2.17), i.e.

$$\rho(t, x) := |\psi(t, x)|^2 \equiv |\psi(t_n, x)|^2 = \rho(t_n, x), \quad t \geq t_n, \quad a \leq x \leq b. \quad (2.19)$$

Plugging (2.19) into (2.17), Eq. (2.17) collapses to a linear ODE as

$$i\varepsilon \partial_t \psi(t, x) = V(x)\psi(t, x) + f(|\psi(t_n, x)|^2)\psi(t, x), \quad a \leq x \leq b, \quad t > t_n, \quad (2.20)$$

which can be integrated *analytically* as

$$\psi(t, x) = e^{-i[V(x)+f(|\psi(t_n, x)|^2)](t-t_n)/\varepsilon} \psi(t_n, x), \quad t \geq t_n, \quad a \leq x \leq b. \quad (2.21)$$

In practical computation, from time $t = t_n$ to $t = t_{n+1}$, one often combines the splitting steps *via* the standard Strang splitting [169] — which is usually referred to as time-splitting sine pseudospectral (TSSP) method [29, 36, 39, 40, 53] — as

$$\begin{aligned} \psi_j^{(1)} &= e^{-i\tau[V(x_j)+f(|\psi_j^n|^2)]/2\varepsilon} \psi_j^n, \\ \psi_j^{(2)} &= \sum_{l=1}^{J-1} e^{-i\tau\varepsilon\mu_l^2/2} (\widehat{\psi}^{(1)})_l \sin(\mu_l(x_j - a)) = \sum_{l=1}^{J-1} e^{-i\tau\varepsilon\mu_l^2/2} (\widehat{\psi}^{(1)})_l \sin\left(\frac{l j \pi}{J}\right), \\ \psi_j^{n+1} &= e^{-i\tau[V(x_j)+f(|\psi_j^{(2)}|^2)]/2\varepsilon} \psi_j^{(2)}, \quad 1 \leq j \leq J-1, \quad n \geq 0, \end{aligned} \quad (2.22)$$

where $\psi_0^{n+1} = \psi_j^{n+1} = 0$ for $n \geq 0$, $\psi_j^0 = \psi_0(x_j)$ for $0 \leq j \leq J$, and $(\widehat{\psi}^{(1)})_l$ for $1 \leq l \leq J-1$, the discrete sine transform coefficients of the complex-valued vector $\psi^{(1)} = (\psi_0^{(1)}, \psi_1^{(1)}, \dots, \psi_J^{(1)})^T$ with $\psi_0^{(1)} = \psi_J^{(1)} = 0$, are defined by

$$\mu_l = \frac{\pi l}{b-a}, \quad \widehat{\psi}^{(1)} = \frac{2}{J} \sum_{j=1}^{J-1} \psi_j^{(1)} \sin(\mu_l(x_j - a)) = \frac{2}{J} \sum_{j=1}^{J-1} \psi_j^{(1)} \sin\left(\frac{l j \pi}{J}\right), \quad 1 \leq l \leq J-1. \quad (2.23)$$

Again, the above TSSP method is *time reversible* or *symmetric*, its memory cost is $O(J^d)$ in d -dimensions with J unknowns along each direction. Its implementation is much easier than for CNFD, ReFD and SIFD. It is an explicit scheme since there is no need to solve a linear system and, at each time step, the computational cost is $O(J^d \ln J)$. It conserves the *mass* (2.4) in the discretized level as (2.9) [29, 36, 39, 40, 53], and it is therefore unconditionally stable. In addition, it can be rigorously proven that the TSSP method is second-order accurate in time and spectral order accurate in space for any fixed $\varepsilon = \varepsilon_0 = O(1)$ [29, 62, 113, 139, 151, 168, 175]. In addition, it is *time transverse invariant*, i.e. when $V(x) \rightarrow V(x) + \alpha$ with α a constant, then $\psi_j^n \rightarrow \psi_j^n e^{-ian\tau/\varepsilon}$ which implies that the density $\rho_j^n := |\psi_j^n|^2$ is unchanged; it has the same *dispersion relation* as the NLSE/GPE (2.1), i.e. if $V(x) \equiv 0$ and $\psi_0(x_j) = A e^{ikx_j}$ for $0 \leq j \leq J$, then the numerical solution from the TSSP method is $\psi_j^n = A e^{i(kx_j - \omega t_n)}$ with ω , A and k satisfying the dispersion relation (1.7) provided that $J \geq k$. However, it cannot preserve *energy conservation* properties of the NLSE/GPE (2.1) in the discretized level [39, 40]. In fact, the numerical solution from the TSSP method actually coincides with the exact solution of a modified PDE at each time step. This shows the existence of a modified energy [89, 97, 98, 103, 105] preserved by the numerical scheme that is close to the exact energy if the numerical solution is smooth. However, some resonances may destroy the energy conservation on long time evolution (see Chapter 7 of [103]). Finally, for designing high-order, e.g. fourth-order accurate in time, time-splitting spectral methods, we refer to [45, 53, 174, 175] and references therein.

In the literatures, in some applications where the solution of the NLSE/GPE is not smooth, e.g. with random potential [10, 96, 140, 148], then the following time-splitting finite difference (TSFD) – in which the time-splitting

is applied first and then the free Schrödinger equation (2.16) is discretized by the CNFD method — is used for discretizing the NLSE/GPE [29, 48, 49, 178] as

$$\begin{aligned} \psi_j^{(1)} &= e^{-i\tau[V(x_j)+f(|\psi_j^n|^2)]/2\varepsilon} \psi_j^n, & 0 \leq j \leq J, \\ i\varepsilon \frac{\psi_j^{(2)} - \psi_j^{(1)}}{\tau} &= -\frac{\varepsilon^2}{4} \left[(D_x^2 \psi^{(2)})_j + (D_x^2 \psi^{(1)})_j \right], & 1 \leq j \leq J-1, & \psi_0^{(2)} = \psi_J^{(2)} = 0, \\ \psi_j^{n+1} &= e^{-i\tau[V(x_j)+f(|\psi_j^{(2)}|^2)]/2\varepsilon} \psi_j^{(2)}, & 0 \leq j \leq J, & n \geq 0, \end{aligned} \quad (2.24)$$

where $\psi_j^0 = \psi_0(x_j)$ for $0 \leq j \leq J$. Similarly, the above TSFD method is *time reversible or symmetric*, its memory cost is $O(J^d)$ in d -dimensions with J unknowns in each direction; it is easier to be implemented than CNFD, ReFD and SIFD. It is an implicit scheme where, at each time step, only a linear system (whose coefficient matrix is time independent) needs to be solved, which can be done in $O(J)$ operations in 1D and $O(J^d \ln J)$ operations in 2D/3D. Therefore it is significantly cheaper than the CNFD and ReFD methods. The TSFD method is second-order accurate both in time and space for any fixed $\varepsilon = \varepsilon_0 = O(1)$ [29, 49]. In addition, it conserves the *mass* (2.4) at the discretized level as (2.9) [29, 48, 49] and thus it is unconditionally stable; it is also *time transverse invariant*. However, there is no *energy conservation* property of the NLSE/GPE (2.1) at the discretized level [29, 48, 49].

For comparison and convenience of the readers, we summarize the main physical and computational properties of the above popular numerical methods CNFD, ReFD, SIFD, TSSP and TSFD in Table 1. From this Table, we can see that the TSSP method shares the most properties as the original NLSE/GPE. In addition, it is very efficient and accurate as well as easy to be implemented in practical computations, especially in 2D and 3D [29, 36, 39, 40, 45, 174]. In fact, the TSSP method becomes more and more popular in practical computations, especially in the numerical simulation of Bose-Einstein condensation [29, 36, 45, 124, 125, 174, 176].

Method	TSSP	CNFD	SIFD	ReFD	TSFD
Time Reversible	Yes	Yes	Yes	Yes	Yes
Time Transverse Invariant	Yes	No	No	No	Yes
Mass Conservation	Yes	Yes	No	Yes	Yes
Energy Conservation	No	Yes	No	Yes ⁴	No
Dispersion Relation	Yes	No	No	No	Yes
Unconditional Stability	Yes	Yes	No	Yes	Yes
Explicit Scheme	Yes	No	No	No	No
Time Accuracy	2 th or 4 th	2 th	2 th	2 th	2 th
Spatial Accuracy	spectral	2 th	2 th	2 th	2 th
Memory Cost	$O(J^d)$	$O(J^d)$	$O(J^d)$	$O(J^d)$	$O(J^d)$
Computational Cost	$O(J^d \log J)$	$\gg O(J^d)$ ⁵	$O(J^d \log J)$ ⁶	$O(J^d \log J)$ ⁷	$O(J^d \log J)$ ⁸
Resolution when $0 < \varepsilon \ll 1$ ⁹	$h = O(\varepsilon)$ $\tau = O(\varepsilon)$	$h = o(\varepsilon)$ $\tau = o(\varepsilon)$	$h = o(\varepsilon)$ $\tau = o(\varepsilon)$	$h = o(\varepsilon)$ $\tau = o(\varepsilon)$	$h = o(\varepsilon)$ $\tau = o(\varepsilon)$

Table 1. Physical and numerical properties of different popular numerical methods in the d -dimensional case with J unknowns in each direction.

Remark 2.1 If the homogeneous Dirichlet boundary condition (2.2) is replaced by the periodic boundary condition, e.g. for BEC on a ring [29, 39, 40, 49], the above numerical methods are still valid provided that we replace $1 \leq j \leq J-1$ by $0 \leq j \leq J-1$ in all the numerical methods, and replace $\psi_0^{n+1} = \psi_J^{n+1} = 0$ by $\psi_0^{n+1} = \psi_J^{n+1}$ and $\psi_{-1}^{n+1} = \psi_{J-1}^{n+1}$ in the CNFD, ReFD and SIFD methods, the sine basis by the Fourier basis in the TSSP method, and $\psi_0^{(2)} = \psi_J^{(2)} = 0$ by $\psi_0^{(2)} = \psi_J^{(2)}$ and $\psi_{-1}^{(2)} = \psi_{J-1}^{(2)}$ in the TSFD method, respectively. Similarly, if the homogeneous Dirichlet boundary

⁴Only for cubic nonlinearity

⁵Depends on the solver for the nonlinear system

⁶If $d = 1$, $O(J)$

⁷If $d = 1$, $O(J)$

⁸If $d = 1$, $O(J)$

⁹For cubic repulsive nonlinearity

condition (2.2) is replaced by the homogeneous Neumann boundary condition, e.g. for the dynamics of dark solitons and their interaction [26, 29, 49], the above numerical methods are still valid provided that we replace $1 \leq j \leq J-1$ by $0 \leq j \leq J$ in all the numerical methods, and replace $\psi_0^{n+1} = \psi_J^{n+1} = 0$ by $\psi_{-1}^{n+1} = \psi_0^{n+1}$ and $\psi_{J+1}^{n+1} = \psi_{J-1}^{n+1}$ in the CNFD, ReFD and SIFD methods, the sine basis by the cosine basis in the TSSP method, and $\psi_0^{(2)} = \psi_J^{(2)} = 0$ by $\psi_{-1}^{(2)} = \psi_0^{(2)}$ and $\psi_{J+1}^{(2)} = \psi_{J-1}^{(2)}$ in the TSFD method, respectively [26, 29, 49]. Then the physical and numerical properties of these numerical methods are still valid.

2.2. Other numerical methods

In the literatures, there are many other numerical methods proposed for discretizing the NLSE/GPE. For example, Sanz-Serna [99, 160, 163, 164] proposed the following second-order finite difference (SSFD) method which is well-adapted to the computation of soliton-like solutions of NLSE/GPE

$$i\varepsilon \frac{\psi_j^{n+1} - \psi_j^n}{\tau} = -\frac{\varepsilon^2}{4} \left[(D_x^2 \psi^{n+1})_j + (D_x^2 \psi^n)_j \right] + \left[V(x_j) + f \left(\left| \frac{\psi_j^{n+1} + \psi_j^n}{2} \right|^2 \right) \right] \frac{\psi_j^{n+1} + \psi_j^n}{2}, \quad 1 \leq j \leq J-1, \quad n \geq 0, \quad (2.25)$$

and the boundary and initial conditions (2.2)-(2.3) are discretized as (2.8). Another one is the leap-frog finite difference (LPFD) method as [150, 190]

$$i\varepsilon \frac{\psi_j^{n+1} - \psi_j^{n-1}}{2\tau} = -\frac{\varepsilon^2}{2} (D_x^2 \psi^n)_j + \left[V(x_j) + f \left(|\psi_j^n|^2 \right) \right] \psi_j^n, \quad 1 \leq j \leq J-1, \quad n \geq 1, \quad (2.26)$$

and the boundary and initial conditions (2.2)-(2.3) are discretized as (2.8) and the first step can be computed as (2.15). In fact, in the physics literatures, for time discretization, the fourth-order Runge-Kutta (RK4) method was also used [4, 24, 70, 69], which is not time symmetric. Thus, in general, it should be avoid to use RK4 for solving the NLSE/GPE. In some mathematics literatures, for space discretization, the 4th-order compact finite difference method has been used [138, 184] and the finite element (FE) method was also developed and analyzed [8, 9]. However, since the computational domains for NLSE/GPE are usually simple and regular, the FE method for spatial discretization is usually not adapted in practical computations. Last but not the least, we want to mention that, in some physics papers, for solving NLSE/GPE in 2D or 3D, the alternating direction implicit (ADI) is first adapted to decouple the NLSE/GPE into dimension-by-dimension and then the SIFD or CNFD is used to discretize each NLSE/GPE in 1D [4, 100, 111, 150, 161, 162]. For other more numerical methods for NLSE/GPE, we refer to [7, 22, 24, 26, 75, 76, 77, 78, 82, 91, 93, 95, 106, 110, 117, 121, 122, 123, 126, 127, 128, 136, 150, 160, 161, 183] and references therein. In general, these numerical methods have less good properties as those methods mentioned in the previous subsection and thus we omit the details here for brevity.

2.3. Perfectly matched layers and/or absorbing boundary conditions

In some situations for solving the NLSE/GPE (1.1) numerically, e.g. very long time dynamics and the potential is not a confinement potential in nonlinear optics [21, 23], the simple boundary condition, such as homogeneous Dirichlet or Neumann or periodic boundary condition used in the previous subsections to truncate (or approximate) the original NLSE/GPE from the whole space problem to a bounded computational domain, might bring large truncation errors except that the bounded computational domain is chosen extremely large and/or time-dependent. Thus, in order to choose a smaller computational domain which might save memory and/or computational cost, perfectly matched layers (PMLs) [60] or high-order absorbing (or artificial) boundary conditions (ABCs) [12, 21, 23, 59, 102, 149, 154] need to be designed and/or used at the artificial boundary so that one can truncate (or approximate) the original NLSE/GPE into a smaller bounded computational domain. Over the last 20 years, different PMLs [153, 195] and/or ABCs [14, 15, 16, 17, 18, 19, 21, 23, 172, 171, 194] have been designed for solving the NLSE/GPE in the literatures. Here we simply review some of them for the completeness of this paper.

In fact, PMLs were introduced by Bérenger in 1994 for electromagnetic field computations [60] and they have been extended to NLSE/GPE by various authors recently [153, 195]. Again, here we present the idea in 1D. Suppose that one is only interested in the solution of the NLSE/GPE (1.1) with $d = 1$ over the physical domain (a, b) . One introduces two layers with width $R_0 > 0$ at $x = a$ and $x = b$ and defines the following function

$$S(x) := 1 + R\sigma(x), \quad \tilde{a} := a - R_0 \leq x \leq b + R_0 := \tilde{b},$$

where $R \in \mathbb{C}$ and $\sigma(x)$ is a real-valued function which must be chosen properly and very carefully. The goal is to artificially damp the wave traveling inside the two layers to zero without modifying their dynamics in (a, b) by properly chosen R and $\sigma(x)$ [12, 21, 153, 195]. Different choices have been proposed in the literatures [12, 153, 195]. Among them, the following choice works well for the NLSE/GPE (1.1) in 1D with cubic focusing nonlinearity [12, 153, 195]

$$R = e^{i\pi/4}, \quad \sigma(x) = \frac{1}{\delta^2} \begin{cases} (x-a)^2, & \tilde{a} \leq x < a, \\ 0, & a \leq x \leq b, \\ (x-b)^2, & b < x \leq \tilde{b}, \end{cases} \quad (2.27)$$

where δ is a positive constant. Then, the NLSE/GPE (1.1) with $d = 1$ will be truncated (or approximated) as

$$i\varepsilon \partial_t \psi(t, x) = -\frac{\varepsilon^2}{2} \frac{1}{S(x)} \partial_x \left(\frac{1}{S(x)} \partial_x \psi(t, x) \right) + V(x) \psi(t, x) + f(|\psi(t, x)|^2) \psi(t, x), \quad \tilde{a} < x < \tilde{b}, \quad t > 0, \quad (2.28)$$

$$\psi(t, \tilde{a}) = \psi(t, \tilde{b}) = 0, \quad t \geq 0, \quad (2.29)$$

$$\psi(t = 0, x) = \psi_0(x), \quad \tilde{a} \leq x \leq \tilde{b}. \quad (2.30)$$

The above problem can be discretized by CNFD, SIFD, ReFD and TSFD methods straightforward provided that we introduce the following finite difference operator to approximate $\frac{1}{S(x)} \partial_x \left(\frac{1}{S(x)} \partial_x d(x) \right) \Big|_{x=x_j}$ as

$$\frac{1}{S(x)} \partial_x \left(\frac{1}{S(x)} \partial_x d(x) \right) \Big|_{x=x_j} \approx \frac{1}{2h^2 S_j} \left[\frac{1}{S_{j-1/2}} d_{j-1} - \left(\frac{1}{S_{j-1/2}} + \frac{1}{S_{j+1/2}} \right) d_j + \frac{1}{S_{j+1/2}} d_{j+1} \right],$$

where $S_j = S(x_j)$, $S_{j-1/2} = S(x_j - h/2)$ and d_j is the approximation of $d(x_j)$. This PML can be efficient and accurate for the NLSE/GPE in 1D in some cases if one can choose δ and R_0 properly. Of course, extensions to 2D and 3D are a little bit more difficult and it might give bad numerical results or even not work in some situations when one chooses improper layer function $S(x)$ and/or layer width R_0 . Another way to design the PML is to introduce a damping potential which is also called as complex absorbing potential (CAP) or exterior complex scaling (ECS) [134, 166], i.e. choosing $S(x) \equiv 1$ for $\tilde{a} \leq x \leq \tilde{b}$ and replacing the real-valued potential $V(x)$ by a complex-valued potential $\tilde{V}(x) := V(x) - i\sigma(x)$, where $\sigma(x)$ is given in (2.27) with δ and σ_0 two real constants to be determined based on the application. Then, the problem can be discretized by TSSP, CNFD, SIFD, ReFD and TSFD methods straightforwardly. Again, this CAP or ECS can be efficient and accurate for the NLSE/GPE in 1D in some situations if one can choose δ and R_0 suitably. The extensions to the 2D and 3D cases are direct. It might also lead to large inaccuracies in the calculations, more particularly for nonlinear problems. In general, PMLs are more robust from the accuracy point of view [16].

Another way is to find the Dirichlet-to-Neumann (DtN) map for the Schrödinger operator without and/or with external potential and nonlinearity at the boundary of the bounded computational domain by using the continuous and/or discrete Laplace transform [12, 13, 14, 15, 17, 18, 19, 21, 155]. The DtN map is usually nonlocal and a time-dependent pseudo-differential operator, and thus its approximations which involve time fractional derivatives and integrals, are usually used in practical computations. These boundary conditions are also called as absorbing (or artificial or transparent) boundary conditions according to their properties. The goal is to avoid or at least to minimize the wave reflected back inside the domain while it should be outgoing. Since there are several very nice review papers on this part, we omit the details here for brevity and refer to [12] and references therein. Due to the nonlocal ABCs at the artificial boundary, one can usually solve the problem on the bounded computational domain by the second-order finite difference, such as ReFD or SIFD method. It is usually very hard to design spectral order method in space for the NLSE/GPE with nonlocal ABCs.

For comparison of the performance and effectiveness of different PMLs and/or ABCs for NLSE/GPE and their applications, we refer to [17, 135, 186, 187, 189] and references therein.

2.4. Numerical methods in the semi-classical regime

When $0 < \varepsilon \ll 1$ in the NLSE/GPE (1.1), i.e. in the semiclassical limit regime, then the solution propagates waves with wave-length at $O(\varepsilon)$ in both space and time [39, 40, 71, 114, 124, 130]. The highly oscillatory nature

brings severe numerical burdens in numerical computation of the solution of the NLSE/GPE (1.1) [83, 124, 130]. In fact, in order to capture numerically "correct" physical observables such as density and current, different numerical methods request different mesh strategies (or ε -scalability) for discretizing the NLSE/GPE (1.1) in the semiclassical limit regime, i.e. $0 < \varepsilon \ll 1$. Based on the analysis and extensive numerical studies [39, 40, 124, 130], it has been found that the ε -scalability for TSSP is mesh size $h = O(\varepsilon)$, and time step $\tau = O(1)$ -independent of ε and $\tau = O(\varepsilon)$ for the linear Schrödinger equation and NLSE/GPE, respectively; for the CNFD, ReFD, SIFD and TSFD as well as many other finite difference methods, the mesh size is $h = o(\varepsilon)$ and the time step is $\tau = o(\varepsilon)$ [39, 40, 130, 144, 145]. Thus, among those numerical methods for discretizing the NLSE/GPE (1.1) directly, the TSSP method has the best resolution in the semiclassical limit regime.

Of course, there are many other efficient and accurate numerical methods for solving the NLSE/GPE (1.1) based on the oscillatory structure of the solution. For the linear Schrödinger equation, the Gaussian beam method [104, 130, 132, 133, 137, 159] shows good resolution in spatial discretization, which in general requires $h = O(\sqrt{\varepsilon})$ and $\tau = O(1)$ -independent of ε . For the details of the Gaussian beam method, we refer to a recent nice review paper [130] and references therein. However, in general, the Gaussian beam method cannot be extended to deal with the NLSE/GPE (1.1) due to the fact that the superposition is used in the method. We also mention here that there are some numerical methods in the literatures for solving the linear Schrödinger equation based on the Liouville equation through the Wigner transform, which can give good results in the linear case in the semiclassical limit regime [83, 114, 130].

Another approach for dealing with the nonlinear (or linear) Schrödinger equation (1.1) in the semiclassical limit regime is through the Madelung (or WKB) expansion [141, 71]. In the semiclassical limit regime, i.e. $0 < \varepsilon \ll 1$, we denote the solution ψ to the NLSE/GPE (1.1) as ψ^ε and use the following WKB ansatz (or Madelung transformation) [71, 130, 141]

$$\psi^\varepsilon(t, \mathbf{x}) = \sqrt{\rho^\varepsilon(t, \mathbf{x})} \exp\left(\frac{i S^\varepsilon(t, \mathbf{x})}{\varepsilon}\right), \quad \mathbf{x} \in \mathbb{R}^d, \quad t \geq 0, \quad (2.31)$$

where the real-valued functions $\rho^\varepsilon = |\psi^\varepsilon|^2$ and S^ε are the density and phase, respectively. Plugging the above WKB ansatz into the NLSE/GPE (1.1) and identifying real and imaginary parts, the NLSE/GPE is reformulated as a coupled system for density and quantum velocity $v^\varepsilon = \nabla S^\varepsilon$, which is known as quantum hydrodynamic (QHD) system (made of a compressible, isentropic Euler system with Bohm potential) [71, 72]. This model was used in [22, 72, 83, 90, 129] to build an asymptotic preserving (AP) scheme which allows to compute numerical solution with time step and mesh size independent of ε . However, the QHD system fails to represent the solution of the original NLSE/GPE near vacuum, i.e. $\rho^\varepsilon = 0$ [71, 72], and thus the scheme in [90] suffers from difficulties when the density ρ^ε vanishes in the domain and/or shocks or sharp changes happen in the QHD system. To overcome this drawback in the Madelung (or WKB) expansion for including vacuum, Grenier [116] introduced a modified Madelung (or WKB) expansion with the following ansatz [116, 71]

$$\psi^\varepsilon(t, \mathbf{x}) = A^\varepsilon(t, \mathbf{x}) \exp\left(\frac{i S^\varepsilon(t, \mathbf{x})}{\varepsilon}\right), \quad \mathbf{x} \in \mathbb{R}^d, \quad t \geq 0, \quad (2.32)$$

where $A^\varepsilon := a^\varepsilon + i b^\varepsilon$ is a complex-valued function with a^ε and b^ε two real-valued functions. Plugging (2.32) into the NLSE/GPE (1.1) and collecting $O(1)$ and $O(\varepsilon)$ -terms, one obtains a system for A^ε and S^ε (or $v^\varepsilon = \nabla S^\varepsilon$) [71, 116]. Based on this formulation, an AP scheme was proposed in [73], which works up to the time when caustics happens. More recently, another AP scheme [63, 129] was presented based on the Grenier's expansion with a regularized term, which can work after the caustics happens. For more details, we refer to [63, 73] and references therein.

3. Extension to NLSE/GPE with damping and angular rotation terms

3.1. For damped NLSE/GPE

As proven in [29, 74, 170], finite time blow-up may happen for the NLSE/GPE (1.1) with a focusing nonlinearity, e.g. the cubic nonlinearity (1.3) with $\beta < 0$ in 2D/3D. However, the physical quantities modeled by $\psi := \psi(t, \mathbf{x})$ do not become infinite, e.g. in BEC, which implies that the validity of (1.1) breaks down near the singularity. Additional physical mechanisms, which were initially small, become important near the singular point and prevent the formation of the singularity [94, 108, 109]. In BEC, the particle density $\rho := |\psi|^2$ becomes large close to the critical point

and inelastic collisions between particles which are negligible for small densities become important [35, 94, 108, 109]. Therefore, a small damping (absorption) term is introduced into the NLSE/GPE (1.1) which describes inelastic processes [29, 35, 37, 94, 108, 109]. We are interested in the cases where these damping mechanisms are important and, therefore, restrict ourselves to the case of focusing nonlinearity, i.e. $\beta < 0$, where β may also be time dependent. We consider the following damped NLSE/GPE [29, 35, 37, 108, 109]

$$i \partial_t \psi(t, \mathbf{x}) = -\frac{1}{2} \nabla^2 \psi(t, \mathbf{x}) + V(\mathbf{x}) \psi(t, \mathbf{x}) + f(|\psi(t, \mathbf{x})|^2) \psi(t, \mathbf{x}) - i g(|\psi(t, \mathbf{x})|^2) \psi(t, \mathbf{x}), \quad t > 0, \quad \mathbf{x} \in \mathbb{R}^d, \quad (3.1)$$

$$\psi(t = 0, \mathbf{x}) = \psi_0(\mathbf{x}), \quad \mathbf{x} \in \mathbb{R}^d, \quad (3.2)$$

where $g(\rho) \geq 0$ for $\rho := |\psi|^2 \geq 0$ is a real-valued monotonically increasing function.

The general form of (3.1) covers many damped NLSE/GPE arising in various different applications. In BEC, for example, when $g(\rho) \equiv 0$, (3.1) reduces to the usual NLSE/GPE (1.1); a linear damping term $g(\rho) \equiv \delta$ with $\delta > 0$ describes inelastic collisions with the background gas; cubic damping $g(\rho) = \delta_1 \rho$ with $\delta_1 > 0$ corresponds to two-body loss [162]; and a quintic damping term of the form $g(\rho) = \delta_2 \rho^2$ with $\delta_2 > 0$ adds three-body loss to the NLSE/GPE (1.1) [162]. It is easy to see that the decay of the mass according to (3.1) due to damping is given by

$$\dot{N}(t) = \frac{d}{dt} \int_{\mathbb{R}^d} |\psi(t, \mathbf{x})|^2 d\mathbf{x} = -2 \int_{\mathbb{R}^d} g(|\psi(t, \mathbf{x})|^2) |\psi(t, \mathbf{x})|^2 d\mathbf{x} \leq 0, \quad t > 0. \quad (3.3)$$

Particularly, if $g(\rho) \equiv \delta$ with $\delta > 0$, the mass is given by

$$N(t) = \int_{\mathbb{R}^d} |\psi(t, \mathbf{x})|^2 d\mathbf{x} = e^{-2\delta t} N(0) = e^{-2\delta t} \int_{\mathbb{R}^d} |\psi_0(\mathbf{x})|^2 d\mathbf{x}, \quad t \geq 0. \quad (3.4)$$

Due to the appearance of the damping term, new ideas are needed to deal with them and different numerical methods have been presented in the literatures [35, 37]. In fact, the numerical methods such as TSSP, CNFD, ReFD, SIFD and TSFD methods for the NLSE/GPE (1.1) presented in the previous section can be easily extended to the damped NLSE/GPE (3.1). For simplicity of notations, here we only present the TSSP method for (3.1) with quintic damping term in 1D, i.e. $d = 1$ and $g(\rho) = \delta_2 \rho^2$ with $\delta_2 > 0$. From time $t = t_n$ to time $t = t_{n+1}$, the damped NLSE/GPE (3.1) is solved in two steps. One solves

$$i \partial_t \psi(t, x) = -\frac{1}{2} \partial_{xx} \psi(t, x), \quad a < x < b, \quad t > t_n, \quad (3.5)$$

with homogeneous Dirichlet boundary condition for one time step of length τ , followed by solving

$$i \partial_t \psi(t, x) = V(x) \psi(t, x) + f(|\psi(t, x)|^2) \psi(t, x) - i \delta_2 |\psi(t, x)|^4 \psi(t, x), \quad a \leq x \leq b, \quad t > t_n, \quad (3.6)$$

for the same time step τ . Again, Eq. (3.5) is discretized in space by the sine-spectral method and integrated in time *exactly*. For $t \in [t_n, t_{n+1}]$, multiplying the ODE (3.6) by $\bar{\psi}(t, x)$ and then subtracting from its conjugate, we obtain for $\rho(t, x) := |\psi(t, x)|^2$ [35]

$$\partial_t \rho(t, x) = -2\delta_2 \rho^3(t, x), \quad t > t_n, \quad a \leq x \leq b, \quad (3.7)$$

which can be solved analytically as

$$\rho(t, x) = \frac{\rho(t_n, x)}{\sqrt{4\delta_2(t - t_n) + \rho^2(t_n, x)}}, \quad t \geq t_n, \quad a \leq x \leq b. \quad (3.8)$$

Plugging (3.8) into (3.6), we get a linear ODE as

$$i \partial_t \psi(t, x) = \left[V(x) + f\left(\frac{\rho(t_n, x)}{\sqrt{4\delta_2(t - t_n) + \rho^2(t_n, x)}}\right) - i \delta_2 \frac{\rho^2(t_n, x)}{4\delta_2(t - t_n) + \rho^2(t_n, x)} \right] \psi(t, x), \quad t > t_n, \quad a \leq x \leq b, \quad (3.9)$$

which can be integrated *exactly* as for $0 \leq s \leq \tau$ and $a \leq x \leq b$

$$\psi(t_n + s, x) = \psi(t_n, x) \exp \left[-i \left(V(x)s + \frac{i}{4} \rho^2(t_n, x) \ln \frac{\rho^2(t_n, x)}{4\delta_2 s + \rho^2(t_n, x)} + \int_0^s f\left(\frac{\rho(t_n, x)}{\sqrt{4\delta_2 u + \rho^2(t_n, x)}}\right) du \right) \right]. \quad (3.10)$$

For cubic nonlinearity, the last term in the above equation can be integrated *analytically*. For a more general nonlinearity, if it cannot be integrated analytically, one can use a numerical quadrature, e.g. the Simpson's rule, to evaluate it numerically [35, 37]. Then, we can construct the second-order time-splitting sine pseudospectral (TSSP) method for the damped NLSE/GPE (3.1) *via* the Strang splitting [35, 37]; the details are omitted here for brevity.

3.2. NLSE/GPE with an angular rotation term

In view of potential applications of BEC, the study of quantized vortices, which are related to superfluid properties, is one of the key issues. Currently, one of the most popular ways to generate quantized vortices from BEC ground state is the following: impose a laser beam rotating with an angular velocity on the magnetic trap holding the atoms to create a harmonic anisotropic potential. Various experiments have confirmed the observation of quantized vortices in BEC under a rotational frame [3, 5, 6, 29, 70, 142]. At temperatures T much smaller than the critical temperature T_c , BEC in a rotational frame is well described by the macroscopic wave function $\psi := \psi(t, \mathbf{x})$, whose evolution is governed by the following dimensionless GPE with an angular momentum term around the z -axis [5, 6, 29, 45, 50, 107, 158]:

$$i \partial_t \psi(t, \mathbf{x}) = -\frac{1}{2} \nabla^2 \psi(t, \mathbf{x}) + V(\mathbf{x}) \psi(t, \mathbf{x}) + \beta |\psi(t, \mathbf{x})|^2 \psi(t, \mathbf{x}) - \Omega L_z \psi(t, \mathbf{x}), \quad \mathbf{x} \in \mathbb{R}^d, \quad t > 0, \quad (3.11)$$

with initial data

$$\psi(t = 0, \mathbf{x}) = \psi_0(\mathbf{x}), \quad \mathbf{x} \in \mathbb{R}^d, \quad (3.12)$$

where $d = 2$ or 3 for 2D and 3D, respectively, β is a dimensionless constant describing the interaction strength, $V := V(\mathbf{x})$ is a given real-valued potential which is usually chosen as a harmonic potential, Ω is the dimensionless rotation velocity, and

$$L_z = -i(x\partial_y - y\partial_x) \quad (3.13)$$

is the z -component of the angular momentum operator $\mathbf{L} = (L_x, L_y, L_z)^T$ given by $\mathbf{L} = \mathbf{x} \wedge \mathbf{P}$, with the momentum $\mathbf{P} = -i\nabla$. The appearance of the angular momentum term means that we are using a reference frame where the trap is at rest. The above GPE is *time reversible* and *time transverse invariant* and it conserves the *mass* (1.4) and the *energy* defined as [5, 6, 29, 45, 50, 107, 158]

$$E(t) := \int_{\mathbb{R}^d} \left[\frac{1}{2} |\nabla \psi(t, \mathbf{x})|^2 + V(\mathbf{x}) |\psi(t, \mathbf{x})|^2 + \frac{\beta}{2} |\psi(t, \mathbf{x})|^4 - \overline{\Omega \psi(t, \mathbf{x})} L_z \psi(t, \mathbf{x}) \right] d\mathbf{x} \equiv E(0), \quad t \geq 0. \quad (3.14)$$

Due to the appearance of the angular momentum term, new difficulties are introduced in solving the GPE (3.11) for rotating BEC numerically. Several efficient and accurate numerical methods have been proposed in the literatures for discretizing it [29, 31, 34, 41, 42, 50, 70, 162]. In fact, the numerical methods such as TSSP, CNFD, ReFD, SIFD and TSFD methods for the NLSE/GPE (1.1) presented in the previous section can be easily extended to the GPE (3.11) with an angular momentum rotation. For conciseness, we only present here the TSSP method for (3.11) in 2D, i.e. $d = 2$.

From time $t = t_n$ to $t = t_{n+1}$, the GPE (3.11) is solved in two steps. One solves

$$i \partial_t \psi(t, \mathbf{x}) = -\frac{1}{2} \nabla^2 \psi(t, \mathbf{x}) - \Omega L_z \psi(t, \mathbf{x}), \quad t > t_n, \quad (3.15)$$

for one time step of length τ , followed by solving the ODE

$$i \partial_t \psi(t, \mathbf{x}) = V(x) \psi(t, \mathbf{x}) + \beta |\psi(t, \mathbf{x})|^2 \psi(t, \mathbf{x}), \quad t > t_n, \quad (3.16)$$

for the same time step τ . Similar to (2.17), Eq. (3.16) can be solved *analytically* [29, 34]. Some numerical methods have been presented for discretizing (3.15). One numerical method is to adapt the polar coordinates (r, θ) in 2D such that the angular momentum rotation becomes constant coefficient, and then to discretize it in the θ -direction by the Fourier spectral method, in the r -direction by the second-order or fourth-order finite difference method or finite

element method, and in time by the Crank-Nicolson method. For more details, we refer to [29, 34]. Another method is to apply the Alternating Direction Implicit (ADI) method to decouple (3.15) into two sub-problems as

$$i \partial_t \psi(t, \mathbf{x}) = -\frac{1}{2} \partial_{xx} \psi(t, \mathbf{x}) - i \Omega y \partial_x \psi(t, \mathbf{x}), \quad t > t_n, \quad (3.17)$$

$$i \partial_t \psi(t, \mathbf{x}) = -\frac{1}{2} \partial_{yy} \psi(t, \mathbf{x}) + i \Omega x \partial_y \psi(t, \mathbf{x}), \quad t > t_n. \quad (3.18)$$

Now the first problem (3.17) is constant coefficient with respect to x and the second problem (3.17) is constant coefficient with respect to y , and thus they can be discretized in space by the Fourier spectral method and integrated in time *exactly*. Again, for more details, we refer to [29, 50].

A different way to apply the time-splitting technique to the GPE (3.11) is the following: from time $t = t_n$ to time $t = t_{n+1}$, one solves

$$i \partial_t \psi(t, \mathbf{x}) = -\frac{1}{2} \nabla^2 \psi(t, \mathbf{x}) + \frac{|\mathbf{x}|^2}{2} \psi(t, \mathbf{x}) - \Omega L_z \psi(t, \mathbf{x}), \quad \mathbf{x} \in \mathbb{R}^2, \quad t > t_n, \quad (3.19)$$

for one time step of length τ , followed by solving

$$i \partial_t \psi(t, \mathbf{x}) = \left(V(x) - \frac{|\mathbf{x}|^2}{2} \right) \psi(t, \mathbf{x}) + \beta |\psi(t, \mathbf{x})|^2 \psi(t, \mathbf{x}), \quad \mathbf{x} \in \mathbb{R}^2, \quad t > t_n, \quad (3.20)$$

for the same time step τ . Again, similar to (2.17), Eq. (3.20) can be solve *analytically* [29, 41]. Eq. (3.19) can be discretized in space by the generalized-Laguerre-Fourier spectral method and integrated in time *exactly*. One of the advantages of this method is that there is no need to truncate the original GPE (3.11) onto a bounded computational domain. Again, for more details, we refer to [29, 41].

Very recently, a simple and efficient numerical method has been proposed for discretizing the GPE (3.11) *via* a rotating Lagrangian coordinate [20, 42, 112]. For any time $t \geq 0$, let $A(t)$ be an orthogonal rotational matrix defined as

$$A(t) = \begin{pmatrix} \cos(\Omega t) & \sin(\Omega t) \\ -\sin(\Omega t) & \cos(\Omega t) \end{pmatrix}, \quad \text{if } d = 2, \quad (3.21)$$

and

$$A(t) = \begin{pmatrix} \cos(\Omega t) & \sin(\Omega t) & 0 \\ -\sin(\Omega t) & \cos(\Omega t) & 0 \\ 0 & 0 & 1 \end{pmatrix}, \quad \text{if } d = 3. \quad (3.22)$$

It is easy to verify that $A^{-1}(t) = A^T(t)$ for any $t \geq 0$ and $A(0) = I$, with I the identity matrix. For any $t \geq 0$, we introduce the *rotating Lagrangian coordinates* $\tilde{\mathbf{x}}$ as [20, 112]

$$\tilde{\mathbf{x}} = A^{-1}(t) \mathbf{x} = A^T(t) \mathbf{x} \quad \Leftrightarrow \quad \mathbf{x} = A(t) \tilde{\mathbf{x}}, \quad \mathbf{x} \in \mathbb{R}^d, \quad (3.23)$$

and denote the wave function in the new coordinates as $\phi := \phi(t, \tilde{\mathbf{x}})$

$$\phi(t, \tilde{\mathbf{x}}) := \psi(t, \mathbf{x}) = \psi(t, A(t) \tilde{\mathbf{x}}), \quad \mathbf{x} \in \mathbb{R}^d, \quad t \geq 0. \quad (3.24)$$

In fact, here we refer the Cartesian coordinates (t, \mathbf{x}) as the *Eulerian coordinates* and $(t, \tilde{\mathbf{x}})$ to as the rotating Lagrangian coordinates for any fixed $t \geq 0$. Using the chain rule, we obtain the following d -dimensional GPE in the rotating Lagrangian coordinates without the angular momentum rotation term [20, 42]:

$$i \partial_t \phi(t, \tilde{\mathbf{x}}) = \left[-\frac{1}{2} \nabla^2 + W(\tilde{\mathbf{x}}, t) + \beta |\phi|^2 \right] \phi(t, \tilde{\mathbf{x}}), \quad \tilde{\mathbf{x}} \in \mathbb{R}^d, \quad t > 0, \quad (3.25)$$

where $W(\tilde{\mathbf{x}}, t) = V(A(t) \tilde{\mathbf{x}})$ for $\tilde{\mathbf{x}} \in \mathbb{R}^d$ and $t \geq 0$. The initial data (3.12) can be transformed as

$$\phi(t = 0, \tilde{\mathbf{x}}) = \psi(t = 0, \mathbf{x}) = \psi_0(\mathbf{x}) := \phi_0(\mathbf{x}) = \phi_0(\tilde{\mathbf{x}}), \quad \tilde{\mathbf{x}} = \mathbf{x} \in \mathbb{R}^d. \quad (3.26)$$

Then the GPE (3.25) with the initial data (3.26) can be directly solved by the TSSP presented in Section 2. After obtaining the numerical solution $\phi(t, \tilde{\mathbf{x}})$ on a bounded computational domain, if it is needed to recover the original wave function $\psi(t, \mathbf{x})$ over a set of fixed grid points in the Cartesian coordinates \mathbf{x} , one can use the standard Fourier/sine interpolation operators from the discrete numerical solution $\phi(t, \tilde{\mathbf{x}})$ to construct an interpolation continuous function over the bounded computational domain [64, 167], which can be used to compute $\psi(t, \mathbf{x})$ over a set of fixed grid points in the Cartesian coordinates \mathbf{x} for any fixed time $t \geq 0$. For more details, we refer to [42].

4. Extension to coupled NLSEs/GPEs

In many applications, e.g. multi-components BEC [25, 28, 29, 158] and/or interaction of laser beams [1, 2, 55, 152], coupled NLSEs/GPEs have been used for modeling different problems. For simplicity of notations, here we only consider coupled NLSEs/GPEs with two equations and cubic nonlinearity for two-components BEC and/or interaction of two laser beams. Extensions to coupled NLSEs/GPEs with more than two equations are straightforward. Consider [5, 25, 27, 29, 43, 158, 192]

$$\begin{aligned} i\partial_t \psi_1(t, \mathbf{x}) &= \left[-\frac{1}{2} \nabla^2 + V_1(\mathbf{x}) + \beta_{11} |\psi_1|^2 + \beta_{12} |\psi_2|^2 \right] \psi_1 + \lambda \psi_2, & \mathbf{x} \in \mathbb{R}^d, \quad t > 0, \\ i\partial_t \psi_2(t, \mathbf{x}) &= \left[-\frac{1}{2} \nabla^2 + V_2(\mathbf{x}) + \beta_{21} |\psi_1|^2 + \beta_{22} |\psi_2|^2 \right] \psi_2 + \lambda \psi_1, & \mathbf{x} \in \mathbb{R}^d, \quad t > 0, \end{aligned} \quad (4.1)$$

with initial data

$$\psi_1(t=0, \mathbf{x}) = \psi_1^{(0)}(\mathbf{x}), \quad \psi_2(t=0, \mathbf{x}) = \psi_2^{(0)}(\mathbf{x}), \quad \mathbf{x} \in \mathbb{R}^d. \quad (4.2)$$

Here $(\psi_1, \psi_2) := (\psi_1(\mathbf{x}, t), \psi_2(\mathbf{x}, t))$ is the dimensionless complex-valued macroscopic wave function, $V_1(\mathbf{x})$ and $V_2(\mathbf{x})$ are two given dimensionless real-valued external potentials, β_{11} , $\beta_{12} = \beta_{21}$ and β_{22} are given dimensionless real constants describing the interaction strength, and λ is a given dimensionless real constant describing internal atomic Josephson junction in a two-components BEC [25, 27, 29, 158, 179, 180, 192]. This coupled NLSEs/GPEs conserves the *total mass* as [25, 27, 29, 158, 192]

$$N(t) = \int_{\mathbb{R}^d} (|\psi_1(t, \mathbf{x})|^2 + |\psi_2(t, \mathbf{x})|^2) d\mathbf{x} \equiv \int_{\mathbb{R}^d} (|\psi_1^{(0)}(\mathbf{x})|^2 + |\psi_2^{(0)}(\mathbf{x})|^2) d\mathbf{x} := N(0), \quad t \geq 0, \quad (4.3)$$

and the *energy* as

$$\begin{aligned} E(t) &:= \int_{\mathbb{R}^d} \left[\frac{1}{2} (|\nabla \psi_1|^2 + |\nabla \psi_2|^2) + V_1(\mathbf{x}) |\psi_1|^2 + V_2(\mathbf{x}) |\psi_2|^2 + \frac{1}{2} \beta_{11} |\psi_1|^4 \right. \\ &\quad \left. + \frac{1}{2} \beta_{22} |\psi_2|^4 + \beta_{12} |\psi_1|^2 |\psi_2|^2 + 2\lambda \cdot \text{Re}(\psi_1 \bar{\psi}_2) \right] d\mathbf{x} \equiv E(0), \quad t \geq 0, \end{aligned} \quad (4.4)$$

where $\text{Re}(f)$ denotes the real part of the function f . In addition, if there is no internal Josephson junction in (4.1), i.e. $\lambda = 0$, the mass of each component is also conserved [25, 27, 29, 158, 192]

$$N_1(t) := \int_{\mathbb{R}^d} |\psi_1(t, \mathbf{x})|^2 d\mathbf{x} \equiv \int_{\mathbb{R}^d} |\psi_1^{(0)}(\mathbf{x})|^2 d\mathbf{x}, \quad N_2(t) := \int_{\mathbb{R}^d} |\psi_2(t, \mathbf{x})|^2 d\mathbf{x} \equiv \int_{\mathbb{R}^d} |\psi_2^{(0)}(\mathbf{x})|^2 d\mathbf{x}, \quad t \geq 0. \quad (4.5)$$

Different efficient and accurate numerical methods have been proposed in the literatures for discretizing the above coupled NLSEs/GPEs [25, 27, 29, 179, 180, 192]. In fact, the extension of the numerical methods TSSP, CNFD, ReFD, SIFD and TSFD for the NLSE/GPE (1.1) presented in Section 2 is direct for the coupled NLSEs/GPEs (4.1). For simplicity of notations, here we only present the TSSP method for (4.1).

From time $t = t_n$ to time $t = t_{n+1}$, the coupled NLSEs/GPEs (4.1) is solved in two steps. One solves

$$\begin{aligned} i\partial_t \psi_1(t, \mathbf{x}) &= -\frac{1}{2} \nabla^2 \psi_1(t, \mathbf{x}) + \lambda \psi_2(t, \mathbf{x}), & t > t_n, \\ i\partial_t \psi_2(t, \mathbf{x}) &= -\frac{1}{2} \nabla^2 \psi_2(t, \mathbf{x}) + \lambda \psi_1(t, \mathbf{x}), & t > t_n, \end{aligned} \quad (4.6)$$

for one time step of length τ , followed by solving

$$\begin{aligned} i\partial_t \psi_1(t, \mathbf{x}) &= \left[V_1(\mathbf{x}) + \beta_{11} |\psi_1(t, \mathbf{x})|^2 + \beta_{12} |\psi_2(t, \mathbf{x})|^2 \right] \psi_1(t, \mathbf{x}), & t > t_n, \\ i\partial_t \psi_2(t, \mathbf{x}) &= \left[V_2(\mathbf{x}) + \beta_{21} |\psi_1(t, \mathbf{x})|^2 + \beta_{22} |\psi_2(t, \mathbf{x})|^2 \right] \psi_2(t, \mathbf{x}), & t > t_n, \end{aligned} \quad (4.7)$$

for the same time step τ . Similar to (2.16), Eq. (4.6) can be discretized in space by sine spectral method and then integrated in time *exactly* [25, 28, 29, 192]. Like for (2.17), for $t \in [t_n, t_{n+1}]$, Eq. (4.7) leaves $\rho_1 := |\psi_1|^2$ and $\rho_2 := |\psi_2|^2$ invariant [25, 29, 192], i.e. $\rho_1(t, \mathbf{x}) \equiv \rho_1(t_n, \mathbf{x})$ and $\rho_2(t, \mathbf{x}) \equiv \rho_2(t_n, \mathbf{x})$ for $t_n \leq t \leq t_{n+1}$ for any fixed \mathbf{x} ; thus (4.7) can be integrated in time *exactly* [25, 28, 29, 192]. Then, we can construct the second-order TSSP method for the coupled NLSEs/GPEs (4.1) *via* the Strang splitting [25, 27, 29, 54, 192]. We omit the details here for brevity.

We remark here that the above TSSP, CNFD, SIFD methods have been extended to solve many other nonlinear dispersive partial differential equations arising from different applications. For details, we refer to the Schrödinger equation with wave operator [30, 32], the Schrödinger-Poisson system [39, 44, 193], the Zakharov system [47, 46, 79, 115, 131], the Klein-Gordon-Schrödinger equations [52], and the Ginzburg-Laudan-Schrödinger equations [191] and references therein.

5. Numerical comparison and applications

5.1. Comparison of different numerical methods

In order to compare the numerical performance and accuracy of different numerical methods, such as TSSP, CNFD, SIFD, ReFD and TSFD, for the NLSE/GPE (1.1), we take $d = 1$, $\varepsilon = 1$, $V(x) \equiv 0$ and $f(\rho) = -\rho$ in (1.1), and the initial data ψ_0 in (1.2) as

$$\psi_0(x) = A \operatorname{sech}(A(x - x_0)) e^{i(vx + \theta_0)}, \quad x \in \mathbb{R},$$

with $A = 2$, $v = 1$ and $x_0 = \theta_0 = 0$. Then the NLSE/GPE (1.1) with (1.2) has the exact bright soliton solution (1.8), i.e. $\psi(t, x) = \psi_B(t, x)$, with $\beta = -1$, $A = 2$, $v = 1$ and $x_0 = \theta_0 = 0$. In our computation, we take the bounded computational domain as the interval (a, b) with $a = -15$ and $b = 20$ and homogeneous Dirichlet boundary condition, which are large enough so that the truncation errors can be ignored. In order to quantify the numerical solution, we use the l^∞ -norm of the error between the numerical solution ψ_j^n and the exact solution $\psi(t_n, x_j)$ as

$$e_\infty^p(t_n) := \max_{0 \leq j \leq J} |\psi(t_n, x_j) - \psi_j^n|, \quad e_\infty^m(t_n) := \max_{0 \leq j \leq J} (|\psi(t_n, x_j)| - |\psi_j^n|), \quad n \geq 0. \quad (5.1)$$

The functions e_∞^p and e_∞^m allow respectively to measure the phase error and the modulus error.

h		$h_0=0.5$	$h_0/2$	$h_0/4$	$h_0/8$	$h_0/16$
CNFD	e_∞^p	2.48	1.87E0	4.28E-1	1.03E-1	2.57E-2
	e_∞^m	1.89	6.98E-1	1.46E-1	3.52E-2	8.68E-3
ReFD	e_∞^p	2.48	1.87E0	4.28E-1	1.03E-1	2.57E-2
	e_∞^m	1.89	6.98E-1	1.46E-1	3.52E-2	8.68E-3
SIFD	e_∞^p	2.48	1.87E0	4.28E-1	1.03E-1	2.57E-2
	e_∞^m	1.89	6.98E-1	1.46E-1	3.52E-2	8.68E-3
TSFD	e_∞^p	2.48	1.87E0	4.28E-1	1.03E-1	2.57E-2
	e_∞^m	1.89	6.98E-1	1.46E-1	3.52E-2	8.68E-3
TSSP	e_∞^p	1.485	3.81E-4	8.63E-9	<1E-9	<1E-9
	e_∞^m	1.408	2.45E-4	4.49E-9	<1E-9	<1E-9

Table 2. Spatial error analysis on errors $e_\infty^{p,m}(t = 5)$ of different numerical methods for the NLSE/GPE (1.1) in 1D under different mesh sizes h .

To test the spatial discretization errors of the different numerical methods, we fix $\tau = 10^{-5}$ such that the time discretization errors are negligible. Table 2 shows the spatial errors $e_\infty^{p,m}(t = 5)$ for different numerical methods under

different mesh sizes h . Similarly, to compare the temporal discretization errors of different numerical methods, we take $h = 3.5 \times 10^{-3}$ to get very small spatial discretization errors. Table 3 shows the temporal errors $e_{\infty}^{p,m}(t = 5)$ for different numerical methods under different time steps τ [49].

τ		$\tau_0=0.1$	$\tau_0/2$	$\tau_0/4$	$\tau_0/8$	$\tau_0/16$
CNFD	e_{∞}^p	2.62E-1	6.65E-2	1.64E-2	3.88E-3	7.28E-4
	e_{∞}^m	1.08E-2	2.87E-3	6.70E-4	1.16E-4	6.64E-5
ReFD	e_{∞}^p	3.11E-1	2.68E-2	1.97E-2	5.07E-3	1.47E-3
	e_{∞}^m	2.25E-1	5.37E-2	1.34E-2	3.37E-3	9.25E-4
SIFD	e_{∞}^p	2.96E0	6.46E-1	1.91E-1	6.62E-2	2.61E-2
	e_{∞}^m	2.57E-1	1.13E-1	5.34E-2	2.58E-2	1.26E-2
TSFD	e_{∞}^p	8.51E-1	2.00E-1	4.97E-2	1.25E-2	3.37E-3
	e_{∞}^m	4.10E-1	9.03E-2	2.20E-2	5.49E-3	1.44E-3
TSSP	e_{∞}^p	5.17E-1	1.40E-1	3.57E-2	8.98E-3	2.25E-3
	e_{∞}^m	4.98E-2	1.64E-2	4.21E-3	1.06E-3	2.65E-4

Table 3. Temporal error analysis on errors $e_{\infty}^{p,m}(t = 5)$ of different numerical methods for the NLSE/GPE (1.1) in 1D under different time steps τ .

From Tabs. 2 & 3 as well as additional numerical results not shown here for brevity, it is clearly demonstrated that TSSP is spectral order accurate in space and second-order accurate in time while CNFD, ReFD, SIFD and TSFD are second-order accurate in both space and time. For more numerical comparisons, we refer to [29, 49, 80] and references therein.

5.2. Applications

In order to show numerical results for problems coming from applications, we consider the dynamics of the NLSE/GPE (3.11) with a rotation term in 2D starting from a quantized vortex lattice for a rotating BEC [29, 31, 41, 42, 50], i.e. we take $d = 2$, $\beta = 1000$ and $\Omega = 0.9$ in (3.11). The initial datum in (3.12) is chosen as a stationary vortex lattice which is computed numerically by using the method in [29, 51] with the above parameters and the harmonic potential $V(x, y) = \frac{1}{2}(x^2 + y^2)$. Then, the dynamics of the vortex lattice is studied numerically by perturbing the harmonic potential from $V(x, y) = \frac{1}{2}(x^2 + y^2)$ to $V(x, y) = \frac{1}{2}(\gamma_x^2 x^2 + \gamma_y^2 y^2)$ with (i) case I: $\gamma_x = \gamma_y = 2$, and (ii) case II: $\gamma_x = 1.1$ and $\gamma_y = 0.9$, respectively, at time $t = 0$. In the numerical simulation, we choose the bounded computational domain as $[-32, 32]^2$ with homogeneous Dirichlet boundary condition, mesh size $h = 1/16$ and time step $\tau = 10^{-4}$. Figure 1 shows the contour plots of the density function $\rho(t, \mathbf{x}) := |\psi(t, \mathbf{x})|^2$ displayed on $[-17, 17]^2$ at different times for cases I and II.

6. Conclusion and perspectives

Due to its massive applications in many different areas, the research on numerical methods and simulation as well as applications related to the nonlinear Schrödinger/Gross-Pitaevskii equations (NLSE/GPE) has been started several decades ago. Up to now, rich and extensive research results have been obtained in developing and analyzing efficient and accurate numerical methods for the NLSE/GPE and in applying them for simulating problems arising from many different areas, such as Bose-Einstein condensation (BEC), nonlinear optics, superfluids, etc. Nowadays, numerical simulation has become a very important tool in theoretical and computational physics as well as computational and applied mathematics for solving problems related to NLSE/GPE and it has been used to predict and guide new experiments due to the advances in numerical methods and their analysis as well as powerful and/or parallel computers. Of course, due to its dispersive nature of the NLSE/GPE, when one is doing numerical simulation, he/she should choose the numerical method, mesh size and time step as well as the computational domain properly and carefully so that the numerical results reflect “correct” physical phenomena.

The research in this area is still very active and highly demanded due to the latest experimental and/or technological advances in BEC, nonlinear optics, graphene, semiconductors, topological insulators, materials simulation and

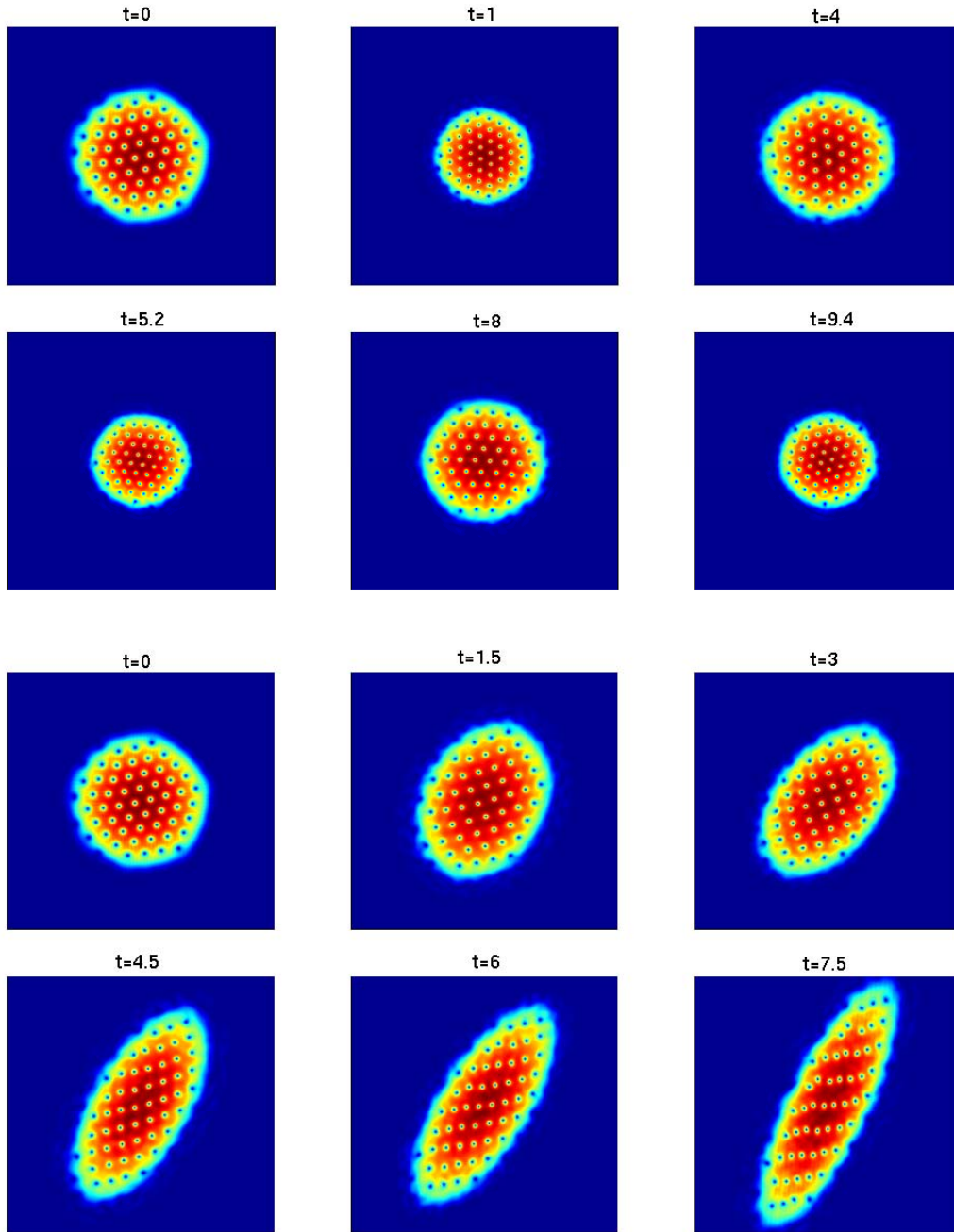


Figure 1. Contour plots of the density function $\rho := |\psi(t, \mathbf{x})|^2$ for the dynamics of a quantized vortex lattice in a rotating BEC for case I (top two rows) and case II (bottom two rows).

design, etc. It becomes more and more interdisciplinary involving theoretical, computational and experimental physicists and computational and applied mathematicians as well as computational scientists. Of course, there are still many important issues to be addressed. For example, extension and designing as well as analyzing new numerical methods for highly oscillatory nonlinear dispersive partial differential equations, especially coupled NLSE/GPE with other equations such as the Davey-Stewartson system [170], Kadomstev-Petiashvili equations [170], coupled NLSE/GPE

with quantum Boltzmann equation for BEC at finite temperature [29, 188], etc., are always welcome and highly demanded. Another issue is to design efficient and accurate numerical methods and apply them for studying numerically NLSE/GPE with random potential [10, 96, 140, 148] or stochastic NLSE/GPE [58, 86, 87, 88, 147] with applications and NLSE/GPE in higher dimensions, i.e. $d > 3$ for many-body problems in quantum chemistry and materials simulation and design. Here memory and computational cost might be extremely high and thus parallel computing and/or sparse grids as well as spatial and temporal adaptivity are very useful and essential. Last but not the least, efficient implementation of numerical methods and portable and readable programming are very important from the application point of view. Although there are plenty of research codes available in the community [67, 68, 150, 177], a software package or tool box (with parallel implementation in 2D and 3D) is still very useful for applications. In summary, in order to solve challenging scientific and engineering problems and/or guiding and predicting new experiments related to NLSE/GPE, the interaction and close collaboration between computational and applied mathematicians and theoretical and experimental physicists and chemists as well as computational and applied scientists becomes more and more essential in this research area.

Acknowledgements.

This work was partially supported by the French ANR grants MicroWave NT09_460489 (“Programme Blanc” call) and ANR-12-MONU-0007-02 BECASIM (“Modèles Numériques” call) (X. Antoine and C. Besse), and by the Singapore A*STAR SERC PSF-Grant 1321202067 (W. Bao).

References

- [1] F. Abdullaev, S. Darmanyan, P. Khabibullaev, *Optical Solitons* (Springer Verlag, New York, 1993).
- [2] M. J. Ablowitz, H. Segur, *Solitons and the Inverse Scattering Transform* (SIAM, Philadelphia, 1981).
- [3] J. R. Abo-Shaeer, C. Raman, J. M. Vogels, W. Ketterle, Observation of vortex lattices in Bose-Einstein condensates, *Science* 292 (2001) 476–479.
- [4] S. K. Adhikari, Numerical study of the spherically symmetric Gross-Pitaevskii equation in two space dimensions, *Phys. Rev. E* 62 (2000) 2937–2944.
- [5] A. Aftalion, *Vortices in Bose-Einstein Condensates* (Birkhäuser, Boston, 2006).
- [6] A. Aftalion, Q. Du, Vortices in a rotating Bose-Einstein condensate: critical angular velocities and energy diagrams in the Thomas-Fermi regime, *Phys. Rev. A* 64 (2001) 063603.
- [7] G. D. Akrivis, Finite difference discretization of the cubic Schrödinger equation, *IMA J. Numer. Anal.* 13 (1993) 115–124.
- [8] G. D. Akrivis, V. A. Dougalis, On a class of conservative, highly accurate Galerkin methods for the Schrödinger equation, *RAIRO Modél. Math. Anal. Numér.* 25 (1991) 643–670.
- [9] G. D. Akrivis, V. A. Dougalis, O. A. Karakashian, On fully discrete Galerkin methods of second-order temporal accuracy for the nonlinear Schrödinger equation, *Numer. Math.* 59 (1991) 31–53.
- [10] P. W. Anderson, Absence of diffusion in certain random lattices, *Phys. Rev. Lett.* 109 (1958) 1492–1505.
- [11] M. H. Anderson, J. R. Ensher, M. R. Matthews, C. E. Wieman, E. A. Cornell, Observation of Bose-Einstein condensation in a dilute atomic vapor, *Science* 269 (1995) 198–201.
- [12] X. Antoine, A. Arnold, C. Besse, M. Ehrhardt, A. Schädle, A review of transparent and artificial boundary conditions techniques for linear and nonlinear Schrödinger equations, *Commun. Comput. Phys.* 4 (2008) 729–796.
- [13] X. Antoine, C. Besse, Unconditionally stable discretization schemes of non-reflecting boundary conditions for the one-dimensional Schrödinger equation, *J. Comput. Phys.* 188 (2003) 157–175.
- [14] X. Antoine, C. Besse, S. Descombes, Artificial boundary conditions for one-dimensional cubic nonlinear Schrödinger equations, *SIAM J. Numer. Anal.* 43 (2006) 2272–2293.
- [15] X. Antoine, C. Besse, P. Klein, Absorbing boundary conditions for the one-dimensional Schrödinger equation with an exterior repulsive potential, *J. Comput. Phys.* 228 (2009) 312–335.
- [16] X. Antoine, C. Besse, P. Klein, Numerical solution of time-dependent nonlinear Schrödinger equations using domain truncation techniques coupled with relaxation scheme, *Laser Physics* 21 (2011) 1191–1502.
- [17] X. Antoine, C. Besse, P. Klein, Absorbing boundary conditions for general nonlinear Schrödinger equations, *SIAM J. Sci. Comput.* 33 (2011) 1008–1033.
- [18] X. Antoine, C. Besse, P. Klein, Absorbing boundary conditions for the two-dimensional Schrödinger equation with an exterior potential: Part I construction and a priori estimates, *Math. Mod. Meth. Appl. Sci.* 22 (2012) 50026–50064.
- [19] X. Antoine, C. Besse, P. Klein, Absorbing boundary conditions for the two-dimensional Schrödinger equation with an exterior potential: Part II discretization and numerical results, *Numer. Math.*, to appear.
- [20] P. Antonelli, D. Marahrens, C. Sparber, On the Cauchy problem for nonlinear Schrödinger equations with rotation, *Disc. Contin. Dyn. Syst. A* 32 (2012) 703–715.
- [21] A. Arnold, Numerically absorbing boundary conditions for quantum evolution equations, *VLSI Design* 6 (1998) 313–319.
- [22] A. Arnold, N. Ben Abdallah, C. Negulescu, WKB-based schemes for the oscillatory 1D Schrödinger equation in the semi-classical limit, *SIAM J. Numer. Anal.* 49 (2011) 1436–1460.

- [23] A. Arnold, M. Ehrhardt, M. Schulte, I. Sofronov, Discrete transparent boundary conditions for the Schrödinger equation on circular domains, *Commun. Math. Sci.* 10 (2012) 889–916.
- [24] R. Baer, Accurate and efficient evolution of nonlinear Schrödinger equations, *Phys. Rev. A* 62 (2000) 063810.
- [25] W. Bao, Ground states and dynamics of multicomponent Bose-Einstein condensates, *Multiscale Model. Simul.* 2 (2004) 210–236.
- [26] W. Bao, Numerical methods for the nonlinear Schrödinger equation with nonzero far-field conditions, *Methods Appl. Anal.*, 11 (2004) 367–387.
- [27] W. Bao, The nonlinear Schrödinger equation and applications in Bose-Einstein condensation and plasma physics, In “Dynamics in Models of Coarsening, Coagulation, Condensation and Quantization” (IMS Lecture Notes Series, World Scientific) 9 (2007) 141–240.
- [28] W. Bao, Analysis and efficient computation for the dynamics of two-component Bose-Einstein condensates: Stationary and time dependent Gross-Pitaevskii equations, *Contemp. Math.* 473 (2008) 1–26.
- [29] W. Bao, Y. Cai, Mathematical theory and numerical methods for Bose-Einstein condensation, *Kinet. Relat. Mod.* 6 (2013) 1–135.
- [30] W. Bao, Y. Cai, Uniform error estimates of finite difference methods for the nonlinear Schrödinger equation with wave operator, *SIAM J. Numer. Anal.* 50 (2012) 492–521.
- [31] W. Bao, Y. Cai, Optimal error estimates of finite difference methods for the Gross-Pitaevskii equation with angular momentum rotation, *Math. Comput.* 82 (2013) 99–128.
- [32] W. Bao, Y. Cai, Uniform and optimal error estimates of an exponential wave integrator sine pseudospectral method for the nonlinear Schrödinger equation with wave operator, *SIAM J. Numer. Anal.*, to appear.
- [33] W. Bao, Y. Cai, H. Wang, Efficient numerical methods for computing ground states and dynamics of dipolar Bose-Einstein condensates, *J. Comput. Phys.* 229 (2010) 7874–7892.
- [34] W. Bao, Q. Du, Y. Zhang, Dynamics of rotating Bose-Einstein condensates and its efficient and accurate numerical computation, *SIAM J. Appl. Math.* 66 (2006) 758–786.
- [35] W. Bao, D. Jaksch, An explicit unconditionally stable numerical method for solving damped nonlinear Schrödinger equations with a focusing nonlinearity, *SIAM J. Numer. Anal.* 41 (2003) 1406–1426.
- [36] W. Bao, D. Jaksch, P. A. Markowich, Numerical solution of the Gross-Pitaevskii equation for Bose-Einstein condensation, *J. Comput. Phys.* 187 (2003) 318–342.
- [37] W. Bao, D. Jaksch, P. A. Markowich, Three dimensional simulation of jet formation in collapsing condensates, *J. Phys. B: At. Mol. Opt. Phys.* 37 (2004) 329–343.
- [38] W. Bao, H. Jian, N. J. Mauser, Y. Zhang, Dimension reduction of the Schrödinger equation with Coulomb and anisotropic confining potentials, preprint.
- [39] W. Bao, S. Jin, P. A. Markowich, On time-splitting spectral approximation for the Schrödinger equation in the semiclassical regime, *J. Comput. Phys.* 175 (2002) 487–524.
- [40] W. Bao, S. Jin, P. A. Markowich, Numerical study of time-splitting spectral discretizations of nonlinear Schrödinger equations in the semiclassical regimes, *SIAM J. Sci. Comput.* 25 (2003) 27–64.
- [41] W. Bao, H.-L. Li, J. Shen, A generalized Laguerre-Fourier-Hermite pseudospectral method for computing the dynamics of rotating Bose-Einstein condensates, *SIAM J. Sci. Comput.* 31 (2009) 3685–3711.
- [42] W. Bao, D. Marahrens, Q. Tang, Y. Zhang, A simple and efficient numerical method for computing the dynamics of rotating Bose-Einstein condensates via a rotating Lagrangian coordinate, preprint.
- [43] W. Bao, P. A. Markowich, C. Schmeiser, R. M. Weishäupl, On the Gross-Pitaevskii equation with strongly anisotropic confinement: formal asymptotics and numerical experiments, *Math. Models Meth. Appl. Sci.* 15 (2005) 767–782.
- [44] W. Bao, N. J. Mauser, H. P. Stimming, Effective one particle quantum dynamics of electrons: A numerical study of the Schrödinger-Poisson- $X\alpha$ model, *Comm. Math. Sci.* 1 (2003) 809–831.
- [45] W. Bao, J. Shen, A fourth-order time-splitting Laguerre-Hermite pseudospectral method for Bose-Einstein condensates, *SIAM J. Sci. Comput.* 26 (2005) 2020–2028.
- [46] W. Bao, F. F. Sun, Efficient and stable numerical methods for the generalized and vector Zakharov system, *SIAM J. Sci. Comput.* 26 (2005) 1057–1088.
- [47] W. Bao, F. F. Sun, G. W. Wei, Numerical methods for the generalized Zakharov system, *J. Comput. Phys.* 190 (2003) 201–228.
- [48] W. Bao, Q. Tang, Numerical study of quantized vortex interaction in nonlinear Schrödinger equation on bounded domain, preprint.
- [49] W. Bao, Q. Tang, Z. Xu, Numerical methods and comparison for computing dark and bright solitons in the nonlinear Schrödinger equation, *J. Comput. Phys.* 235 (2013) 423–445.
- [50] W. Bao, H. Wang, An efficient and spectrally accurate numerical method for computing dynamics of rotating Bose-Einstein condensates, *J. Comput. Phys.* 217 (2006) 612–626.
- [51] W. Bao, H. Wang, P. A. Markowich, Ground, symmetric and central vortex states in rotating Bose-Einstein condensates, *Commun. Math. Sci.* 3 (2005) 57–88.
- [52] W. Bao, L. Yang, Efficient and accurate numerical methods for the Klein-Gordon-Schrödinger equations, *J. Comput. Phys.* 225 (2007) 1863–1893.
- [53] W. Bao, Y. Zhang, Dynamics of the ground state and central vortex states in Bose-Einstein condensation, *Math. Models Methods Appl. Sci.* 15 (2005) 1863–1896.
- [54] W. Bao, Y. Zhang, Dynamical laws of the coupled Gross-Pitaevskii equations for spin-1 Bose-Einstein condensates, *Methods Appl. Anal.* 17 (2010) 49–80.
- [55] W. Bao, C. Zheng, A time-splitting spectral method for three-wave interactions in media with competing quadratic and cubic nonlinearities, *Commun. Comput. Phys.* 2 (2007) 123–140.
- [56] C. Bardos, L. Erdős, F. Golse, N. J. Mauser, H.-T. Yau, Derivation of the Schrödinger-Poisson equation from the quantum N -particle Coulomb problem, *C. R. Math. Acad. Sci. Paris* 334 (2002) 515–520.
- [57] C. F. Barenghi, R. J. Donnelly, W. F. Vinen, *Quantized Vortex Dynamics and Superfluid Turbulence* (Springer, 2001).
- [58] M. Barton-Smith, A. Debussche, L. Di Menza, Numerical study of two-dimensional stochastic NLS equations, *Numer. Methods Partial*

- Differential Equations 21 (2005), (4), 810-842.
- [59] A. Bayliss, E. Turkel, Radiation boundary conditions for wave like equations, *Commun. Pure Appl. Math.* 33 (1980) 707–725.
- [60] J. P. Bérenger, A perfectly matched layer for the absorption of electromagnetic waves, *J. Comput. Phys.* 114 (1994) 185–200.
- [61] C. Besse, A relaxation scheme for the nonlinear Schrödinger equation, *SIAM J. Numer. Anal.* 42 (2004) 934-952.
- [62] C. Besse, B. Bidégary, S. Descombes, Order estimates in time of splitting methods for the nonlinear Schrödinger equation, *SIAM J. Numer. Anal.* 40 (2002) 26–40.
- [63] C. Besse, R. Carles, F. Méhats, An asymptotic preserving scheme based on a new formulation for NLS in the semiclassical limit, arXiv:1211.3391v1.
- [64] J. P. Boyd, A fast algorithm for Chebyshev, Fourier, and sinc interpolation onto an irregular grid, *J. Comput. Phys.* 103 (1992) 243–257.
- [65] Y. Cai, M. Rosenkranz, Z. Lei, W. Bao, Mean-field regime of trapped dipolar Bose-Einstein condensates in one and two dimensions, *Phys. Rev. A* 82 (2010) 043623.
- [66] M. Caliari, Ch. Neuhauser, M. Thalhammer, High-order time-splitting Hermite and Fourier spectral methods for the Gross-CPitaevskii equation *J. Comput. Phys.* 228 (2009) 822C832.
- [67] M. Caliari, S. Rainer, GSGPEs: A MATLAB code for computing the ground state of systems of GrossPitaevskii equations, *Comput. Phys. Commun.*, 184 (2013) (3) pp.812-823.
- [68] R.M. Caplan, NLSEmagic: Nonlinear Schrödinger equation multi-dimensional Matlab-based GPU-accelerated integrators using compact high-order schemes, *Comput. Phys. Commun.*, 184 (2013) (4), pp.1250-1271.
- [69] B. M. Caradoc-Davis, R. J. Ballagh, P. B. Blakie, Three-dimensional vortex dynamics in Bose-Einstein condensates, *Phys. Rev. A* 62 (2000) 011602.
- [70] B. M. Caradoc-Davis, R. J. Ballagh, K. Burnett, Coherent dynamics of vortex formation in trapped Bose-Einstein condensates, *Phys. Rev. Lett.* 83 (1999) 895–898.
- [71] R. Carles, *Semi-Classical Analysis for Nonlinear Schrödinger Equations* (World Scientific, 2008).
- [72] R. Carles, L. Gosse, Numerical aspects of the nonlinear Schrödinger equation in the presence of caustics, *Math. Mod. Meth. Appl. Sci.* 17 (2007) 1531-1553.
- [73] R. Carles and B. Mohammadi, Numerical aspects of the nonlinear Schrödinger equation in the semiclassical limit in a supercritical regime, *ESAIM Math. Model. Numer. Anal.*, 45 (2011), 981–1008.
- [74] T. Cazenave, *Semilinear Schrödinger Equations* (Courant Lect. Notes Math., 10, Amer. Math. Soc., Providence, R.I., 2003).
- [75] M. M. Cerimele, M. L. Chiofalo, F. Pistella, S. Succi, M. P. Tosi, Numerical solution of the Gross-Pitaevskii equation using an explicit finite-difference scheme: An application to trapped Bose-Einstein condensates, *Phys. Rev. E* 62 (2000) 1382–1389.
- [76] M. M. Cerimele, F. Pistella and S. Succi, Particle-inspired scheme for the Gross-Pitaevskii equation: An application to Bose-Einstein condensation, *Comput. Phys. Comm.* 129 (2000) 82–90.
- [77] T. F. Chan, L. Shen, Stability analysis of difference scheme for variable coefficient Schrödinger type equations, *SIAM J. Numer. Anal.* 24 (1987) 336-349.
- [78] T. F. Chan, D. Lee, L. Shen, Stable explicit schemes for equations of the Schrödinger type, *SIAM J. Numer. Anal.* 23 (1986) 274-281.
- [79] Q. Chang, B. Guo, H. Jiang, Finite difference method for generalized Zakharov equations, *Math. Comput.* 64 (1995) 537–553.
- [80] Q. Chang, E. Jia, W. Sun, Difference schemes for solving the generalized nonlinear Schrödinger equation, *J. Comput. Phys.* 148 (1999) 397-415.
- [81] Q. Chang, G. Wang, Multigrid and adaptive algorithm for solving the nonlinear Schrödinger equations, *J. Comput. Phys.* 88 (199) 362.
- [82] Q. Chang, L. Xu, A numerical method for a system of generalized nonlinear Schrödinger equations, *J. Comput. Math.* 4 (1986) 191.
- [83] L.-T. Cheng, H. Liu, S. Osher, Computational high-frequency wave propagation using the level set method, with application to the semiclassical limit of Schrödinger equations, *Comm. Math. Sci.* 1 (2003) 593-621.
- [84] T. Dauxois, M. Peyrard, *Physics of Solitons* (Cambridge University Press, 2006).
- [85] A. S. Davydov, *Solitons in Molecular Systems* (Springer, 1991).
- [86] A. De Bouard, A. Debussche, Weak and strong order of convergence of a semidiscrete scheme for the stochastic nonlinear Schrödinger equation, *Appl. Math. Optim.* 54 (2006), (3), 369-399.
- [87] A. De Bouard, A. Debussche, L. Di Menza, Theoretical and numerical aspects of stochastic nonlinear Schrödinger equations. Monte Carlo and probabilistic methods for partial differential equations (Monte Carlo, 2000). *Monte Carlo Methods Appl.* 7 (2001), (1-2), 55-63.
- [88] A. Debussche, L. Di Menza, Numerical simulation of focusing stochastic nonlinear Schrödinger equations, *Phys. D* 162 (2002), (3-4), 131-154.
- [89] A. Debussche, E. Faou, Modified energy for split-step methods applied to the linear Schrödinger equations, *SIAM J. Numer. Anal.* 47 (2009) 3705–3719.
- [90] P. Degond, S. Gallego, F. Méhats, An asymptotic preserving scheme for the Schrödinger equation in the semiclassical limit, *C. R. Math. Acad. Sci. Paris*, 345 (2007), 531–536.
- [91] M. Delfour, M. Fortin, G. Payre, Finite-difference solutions of a nonlinear Schrödinger equation, *J. Comput. Phys.* 44 (1981) 277-288.
- [92] P. A. M. Dirac, *The Principles of Quantum Mechanics* (Oxford University Press, 1958).
- [93] C. M. Dion, E. Cancès, Spectral method for the time-dependent Gross-Pitaevskii equation with a harmonic trap, *Phys. Rev. E* 67 (2003) 046706.
- [94] E. A. Donley, N. R. Claussen, S. L. Cornish, J. L. Roberts, E. A. Cornell, C. E. Wieman, Dynamics of collapsing and exploding Bose-Einstein condensates, *Nature* 412 (2001) 295-299.
- [95] W. Dörfler, A time- and space-adaptive algorithm for the linear time-dependent Schrödinger equation, *Numer. Math.* 73 (1998) 419-448.
- [96] Y. Dubi, Y. Meir, Y. Avishai, Nature of the superconductor-insulator transition in disordered superconductors, *Nature* 449 (2007) 876-880.
- [97] G. Dujardin, E. Faou, Long time behavior of splitting methods applied to the linear Schrödinger equation, *CR Math. Acad. Sci. Paris* 344 (2007) 89-92.
- [98] G. Dujardin, E. Faou, Normal form and long time analysis of splitting schemes for the linear Schrödinger equation with small potential, *Numer. Math.* 108 (2007) 223-262.

- [99] A. Durán, J. M. Sanz-Serna, The numerical integration of relative equilibrium solutions: the nonlinear Schrödinger equation, *IMA J. Numer. Anal.* 20 (2000) 235–261.
- [100] M. Edwards, K. Burnett, Numerical solution of the nonlinear Schrödinger equation for small samples of neutral atoms, *Phys. Rev. A* 51 (1995) 101103.
- [101] E. D. Engel, M. Reiner, *Density Functional Theory: An Advanced Course* (Springer, 2011).
- [102] B. Engquist, A. Majda, Absorbing boundary conditions for numerical simulation of waves, *Math. Comput.* 31 (1977) 629–651.
- [103] E. Faou, *Geometric Numerical Integration and Schrödinger Equations* (European Mathematical Society, 2012).
- [104] E. Faou, V. Gradinaru, Ch. Lubich, Computing semiclassical quantum dynamics with Hagedorn wavepackets, *SIAM J. Sci. Comput.* 31 (2009) 3027–3041.
- [105] E. Faou, B. Grébert, Hamiltonian interpolation of splitting approximation for Hamiltonian pdes, *Found. Comput. Math.* 11 (2011) 381–415.
- [106] Z. Fei, V. M. Pérez-García, L. Vázquez, Numerical simulation of nonlinear Schrödinger systems: a new conservative scheme, *Appl. Math. Comput.* 71 (1995) 165–177.
- [107] A. L. Fetter, Rotating trapped Bose-Einstein condensates, *Rev. Mod. Phys.* 81 (2009) 647–691.
- [108] G. Fibich, Self-focusing in the damped nonlinear Schrödinger equation, *SIAM J. Appl. Math.* 61 (2001) 1680–1705.
- [109] G. Fibich, G. Papanicolaou, Self-focusing in the perturbed and unperturbed nonlinear Schrödinger equation in critical dimension, *SIAM J. Appl. Math.* 60 (2000) 183–240.
- [110] A. Gammal, T. Frederico, L. Tomio, Improved numerical approach for the time-independent Gross-Pitaevskii nonlinear Schrödinger equation, *Phys. Rev. E* 60 (1999) 2421–2424.
- [111] Z. Gao, S. Xie, Fourth-order alternating direction implicit compact finite difference schemes for two-dimensional Schrödinger equations, *Appl. Numer. Math.* 61 (2011) 595–614.
- [112] J. J. García-Ripoll, V. M. Pérez-García, V. Vekslerchik, Construction of exact solution by spatial translations in inhomogeneous nonlinear Schrödinger equations, *Phys. Rev. E* 64 (2001) 056602.
- [113] L. Gauckler, Ch. Lubich, Splitting integrators for nonlinear Schrödinger equations over long times, *Found. Comput. Math.* 10 (2010) 275–302.
- [114] P. Gerard, P. A. Markowich, N. J. Mauser, F. Poupaud, Homogenization limits and Wigner transforms, *Comm. Pure Appl. Math.* 50 (1997) 321–377.
- [115] R. T. Glassey, Convergence of an energy-preserving scheme for the Zakharov equations in one space dimension, *Math. Comput.* 58 (1992) 83–102.
- [116] E. Grenier, Semiclassical limit of the nonlinear Schrödinger equation in small time, *Proc. Amer. Math. Soc.*, 126 (1998), 523–530.
- [117] D. F. Griffiths, A. R. Mitchell, J. L. Morris, A numerical study of the nonlinear Schrödinger equation, *Comput. Methods Appl. Mech. Engrg.* 45 (1984) 177–215.
- [118] E. P. Gross, Structure of a quantized vortex in boson systems, *Nuovo. Cimento.* 20 (1961) 454–457.
- [119] B. Guo, The convergence of numerical method for nonlinear Schrödinger equation, *J. Comput. Math.* 4 (1986) 121–130.
- [120] R. H. Hardin, F. D. Tappert, Applications of the split-step Fourier method to the numerical solution of nonlinear and variable coefficient wave equations, *SIAM Rev. Chronicle* 15 (1973) 423.
- [121] J. Hong, L. Kong, Novel multi-symplectic integrators for nonlinear fourth-order Schrödinger equation with trapped term, *Commun. Comput. Phys.* 7 (2010) 613C630.
- [122] J. Hong, X.-Y. Liu, C. Li, Multi-symplectic Runge-Kutta-Nyström methods for nonlinear Schrödinger equations with variable coefficients, *J. Comput. Phys.* 226 (2007) 19681984.
- [123] J. Hong, Y. Liu, H. Munthe-Kaas, A. Zanna, Globally conservative properties and error estimation of a multi-symplectic scheme for Schrödinger equations with variable coefficients, *Appl. Numer. Math.* 56 (2006) 814–843.
- [124] Z. Huang, S. Jin, P. A. Markowich, C. Sparber, A Bloch decomposition based numerical method for quantum dynamics in periodic potentials, *SIAM J. Sci. Comput.* 29 (2007) 515–538.
- [125] Z. Huang, S. Jin, P. A. Markowich, C. Sparber, Numerical simulation of the nonlinear Schrödinger equation with multidimensional periodic potentials, *Multiscale Model. Simul.* 7 (2008) 539–564.
- [126] L. I. Ignat, E. Zuazua, Numerical dispersive schemes for the nonlinear Schrödinger equation, *SIAM J. Numer. Anal.* 47 (2009) 1366–1390.
- [127] M. S. Ismail, T. R. Taha, Numerical simulation of coupled nonlinear Schrödinger equation, *Math. Comp. Simul.* 56 (2001) 547–562.
- [128] M. S. Ismail, T. R. Taha, A linearly implicit conservative scheme for the coupled nonlinear Schrödinger equation, *Math. Comp. Simul.* 74 (2007) 302–311.
- [129] S. Jin, H. Liu, S. Osher, T.-H. R. Tsai, Computing multivalued physical observables for the semiclassical limit of the Schrödinger equation, *J. Comput. Phys.* 205 (2005) 222–241.
- [130] S. Jin, P. A. Markowich, C. Sparber, Mathematical and computational methods for semiclassical Schrödinger equations, *Acta Numer.* (2011) 121–209.
- [131] S. Jin, P. A. Markowich, C. Zheng, Numerical simulation of a generalized Zakharov system, *J. Comput. Phys.* 201 (2004) 376–395.
- [132] S. Jin, H. Wu, X. Yang, Gaussian beam methods for the Schrödinger equation in the semi-classical regime: Lagrangian and Eulerian formulations, *Commun. Math. Sci.* 6 (2008) 995–1020.
- [133] S. Jin, H. Wu, X. Yang, Z. Huang, Bloch decomposition-based Gaussian beam method for the Schrödinger equation with periodic potentials, *J. Comput. Phys.* 229 (2010) 4869–4883.
- [134] A. Jüngel, J.F. Mennemann, Time-dependent simulations of quantum waveguides using a time-splitting spectral method, *Math. Comput. Sim.* 81 (2010) 883–898.
- [135] P. Klein, X. Antoine, C. Besse, M. Ehrhardt, Absorbing boundary conditions for solving N-dimensional stationary Schrödinger equations with unbounded potentials and nonlinearities, *Commun. Comput. Phys.* 10 (2011) 1280–1304.
- [136] I. Kyza, C. Makridakis, M. Plexousakis, Error control for time-splitting spectral approximations of the semiclassical Schrödinger equation, *IMA J. Numer. Anal.* 31 (2011) 416–441.
- [137] S. Leung, J. Qian, Eulerian Gaussian beams for the Schrödinger equations in the semi-classical regime, *J. Comput. Phys.* 228 (2009)

- 2951-2977.
- [138] H. Liao, Z. Sun, Error estimate of fourth-order compact scheme for linear Schrödinger equations, *SIAM J. Numer. Anal.* 47 (2010) 4381–4401.
- [139] Ch. Lubich, On splitting methods for Schrödinger-Poisson and cubic nonlinear Schrödinger equations, *Math. Comput.* 77 (2008) 2141–2153.
- [140] J. E. Lye, L. Fallani, M. Modugno, D. S. Wiersma, C. Fort, M. Inguscio, Bose-Einstein condensate in a random potential, *Phys. Rev. Lett.* 95 (2005) 070401.
- [141] E. Madelung, Quantentheorie in hydrodynamischer Form, *Z. Phys.* 40 (1927) 322–326.
- [142] K. W. Madison, F. Chevy, W. Wohlleben, J. Dalibard, Vortex formation in a stirred Bose-Einstein condensate, *Phys. Rev. Lett.* 84 (2000) 806–809.
- [143] P. A. Markowich, *Applied Partial Differential Equations: A Visual Approach* (Springer, 2007).
- [144] P. A. Markowich, P. Pietra, C. Pohl, Numerical approximation of quadratic observables of Schrödinger-type equations in the semi-classical limit, *Numer. Math.* 81 (1999) 595–630.
- [145] P. A. Markowich, P. Pietra, C. Pohl, H. P. Stimming, A Wigner-measure analysis of the Dufort-Fraenkel scheme for the Schrödinger equation, *SIAM J. Numer. Anal.* 40 (2002) 1281–1310.
- [146] P. A. Markowich, C. A. Ringhofer, C. Schmeiser, *Semiconductor Equations* (Springer-Verlag, 2002).
- [147] R. Marty, On a splitting scheme for the nonlinear Schrödinger equation in a random medium, *Commun. Math. Sci.* 4 (4) (2006), 679–705.
- [148] B. Min, T. Li, M. Rosenkranz, W. Bao, Subdiffusive spreading of a Bose-Einstein condensate in random potentials, *Phys. Rev. A* 86 (2012) 053612.
- [149] G. Mur, Absorbing boundary conditions for the finite difference approximation of the time domain electromagnetic field equations, *IEEE Transactions on Electromagnetic Compatibility* 23 (1981) 377–382.
- [150] P. Muruganandam, S. K. Adhikari, Fortran programs for the time-dependent Gross-Pitaevskii equation in a fully anisotropic trap, *Comput. Phys. Commun.* 180 (2009) 1888–1912.
- [151] C. Neuhauser, M. Thalhammer, On the convergence of splitting methods for linear evolutionary Schrödinger equations involving an unbounded potential, *BIT* 49 (2009) 199–215.
- [152] A. C. Newell, *Solitons in Mathematics and Physics* (SIAM, Philadelphia, 1985).
- [153] A. Nissen, G. Kreiss, An optimized perfectly matched layer for the Schrödinger equation, *Commun. Comput. Phys.* 9 (2011) 147–179.
- [154] G. Pang, L. Bian, S. Tang, Almost exact boundary condition for one-dimensional Schrödinger equations, *Phys. Rev. E* 86 (2012) 066709.
- [155] J. S. Papadakis, M. I. Taroudakis, P. J. Papadakis, B. Mayfield, A new method for a realistic treatment of the sea bottom in the parabolic approximation, *J. Acoustical Society of America* 92 (1992) 2030–2038.
- [156] D. Pathria, J. L. Morris, Pseudo-spectral solution of nonlinear Schrödinger equation, *J. Comput. Phys.* 87 (1990) 108–125.
- [157] L. P. Pitaevskii, Vortex lines in an imperfect Bose gas, *Soviet Phys. JETP* 13 (1961) 451–454.
- [158] L. P. Pitaevskii, S. Stringari, *Bose-Einstein Condensation* (Clarendon Press, Oxford, 2003).
- [159] J. Qian, L. Ying, fast Gaussian wavepacket transforms and Gaussian beams for the Schrödinger equation, *J. Comput. Phys.* 229 (2010) 7848–7873.
- [160] M. Robinson, G. Fairweather, B. Herbst, On the numerical cubic Schrödinger equation in one space variable, *J. Comput. Phys.* 104 (1993) 227–284.
- [161] P. A. Ruprecht, M. J. Holland, K. Burnett, M. Edwards, Time-dependent solution of the nonlinear Schrödinger equation for Bose-condensed trapped neutral atoms, *Phys. Rev. A* 51 (1995) 4704–4711.
- [162] H. Saito, M. Ueda, Intermittent implosion and pattern formation of trapped Bose-Einstein condensates with an attractive interaction, *Phys. Rev. Lett.* 86 (2001) 1406–1409.
- [163] J. M. Sanz-Serna, Methods for the numerical solution of the nonlinear Schrödinger equation, *Math. Comput.*, 43 (1984) 21–27.
- [164] J. M. Sanz-Serna, J. G. Verwer, Conservative and nonconservative schemes for the solution of the nonlinear Schrödinger equation, *IMA J. Numer. Anal.* 6 (1986) 25–42.
- [165] E. Schrödinger, An undulatory theory of the mechanics of atoms and molecules, *Phys. Rev.* 28 (1926) 10491070.
- [166] A. Scrinzi, Infinite-range exterior complex scaling as a perfect absorber in time-dependent problems, *Phys. Rev. A* 81 (2010) 053845.
- [167] J. Shen, T. Tang, L. Wang, *Spectral Methods: Algorithms, Analysis and Applications* (Springer, 2011).
- [168] J. Shen, Z.-Q. Wang, Error analysis of the Strang time-splitting Laguerre-Hermite/Hermite collocation methods for the Gross-Pitaevskii equation, *Found. Comput. Math.* 13 (2013) 99–137.
- [169] G. Strang, On the construction and comparison of difference schemes, *SIAM J. Numer. Anal.* 5 (1968) 505–517.
- [170] C. Sulem, P. Sulem, *The Nonlinear Schrödinger Equation: Self-Focusing and Wave Collapse* (Springer, 1999).
- [171] J. Szeftel, Design of absorbing boundary conditions for Schrödinger equations in \mathbb{R}^d , *SIAM J. Numer. Anal.* 42 (2004) 1527–1551.
- [172] J. Szeftel, Absorbing boundary conditions for one-dimensional nonlinear Schrödinger equations, *Numer. Math.* 104 (2006) 103–127.
- [173] T. R. Taha, M. J. Ablowitz, Analytical and numerical aspects of certain nonlinear evolution equations: II numerical, nonlinear Schrödinger equation, *J. Comput. Phys.* 55 (1984) 203–230.
- [174] M. Thalhammer, High-order exponential operator splitting methods for time-dependent Schrödinger equations, *SIAM J. Numer. Anal.* 46 (2008) 2022–2038.
- [175] M. Thalhammer, Convergence analysis of high-order time-splitting pseudo-spectral methods for nonlinear Schrödinger equations, *SIAM J. Numer. Anal.* 50 (2012) 3231–3258.
- [176] M. Thalhammer, J. Abhau, A numerical study of adaptive space and time discretisations for Gross-Pitaevskii equations *J. Comput. Phys.* 231 (2012) 6665–6681.
- [177] D. Vudragovic, I. Vidanovic, A. Balaz, P. Muruganandam, S.K. Adhikari, C programs for solving the time-dependent Gross-Pitaevskii equation in a fully anisotropic trap, *Comput. Phys. Commun.*, 183 (2012) (9), pp. 2021–2025.
- [178] H. Wang, Numerical studies on the split-step finite difference method for nonlinear Schrödinger equations, *Appl. Math. Comp.* 170 (2005), 17–35.
- [179] H. Wang, A time-splitting spectral method for coupled Gross-Pitaevskii equations with applications to rotating Bose-Einstein condensates,

- J. Comput. Appl. Math. 205 (2007) 88–104.
- [180] H. Wang, W. Xu, An efficient numerical method for simulating the dynamics of coupling Bose-Einstein condensates in optical resonators, *Comput. Phys. Comm.* 182 (2011) 706–718.
- [181] T. Wang, Maximum norm error bound of a linearized difference scheme for a coupled nonlinear Schrödinger equations, *J. Comput. Appl. Math.* 25 (2011) 4237–4250.
- [182] J. A. C. Weideman, B. M. Herbst, Split-step methods for the solution of the nonlinear Schrödinger equation, *SIAM J. Numer. Anal.* 23 (1986) 485–507.
- [183] L. Wu, Dufort-Frankel-type methods for linear and nonlinear Schrödinger equations, *SIAM J. Numer. Anal.* 33 (1996) 1526–1533.
- [184] S. Xie, G. Li, S. Yi, Compact finite difference schemes with high accuracy for one-dimensional nonlinear Schrödinger equation, *Comput. Methods Appl. Mech. Engrg.* 198 (2009) 1052–1060.
- [185] B. Xiong, J. Gong, H. Pu, W. Bao, B. Li, Symmetry breaking and self-trapping of a dipolar Bose-Einstein condensate in a double-well potential, *Phys. Rev. A* 79 (2009) 013626.
- [186] Z. Xu, H. Han, Absorbing boundary conditions for nonlinear Schrödinger equations, *Phys. Rev. E* 74 (2006) 037704.
- [187] Z. Xu, H. Han, X. Wu, Adaptive absorbing boundary conditions for Schrödinger-type equations: application to nonlinear and multi-dimensional problems, *J. Comput. Phys.* 225 (2007) 1577–1589.
- [188] E. Zaremba, T. Nikuni, A. Griffin, Dynamics of trapped Bose gases at finite temperature, *J. Low Temp. Phys.* 116 (1999) 277–345.
- [189] J. Zhang, Z. Xu, X. Wu, Unified approach to split absorbing boundary conditions for nonlinear Schrödinger equations: two-dimensional case, *Phys. Rev. E* 79 (2009) 046711.
- [190] Y. Zhang, W. Bao, Dynamics of the center of mass in rotating Bose-Einstein condensates, *Appl. Numer. Math.* 57 (2007) 697–709.
- [191] Y. Zhang, W. Bao, Q. Du, The dynamics and interaction of quantized vortices in Ginzburg-Landau-Schrödinger equations, *SIAM J. Appl. Math.* 67 (2007) 1740–1775.
- [192] Y. Zhang, W. Bao, H.-L. Li, Dynamics of rotating two-component Bose-Einstein condensates and its efficient computation, *Physica D* 234 (2007) 49–69.
- [193] Y. Zhang, X. Dong, On the computation of ground state and dynamics of Schrödinger-Poisson-Slater system, *J. Comput. Phys.* 230 (2011) 2660–2676.
- [194] C. Zheng, Exact nonreflecting boundary conditions for one-dimensional cubic nonlinear Schrödinger equations, *J. Comput. Phys.* 215 (2006) 552–565.
- [195] C. Zheng, A perfectly matched layer approach to the nonlinear Schrödinger wave equations, *J. Comput. Phys.* 227 (2007) 537–556.
- [196] Y. Zhu, Implicit difference scheme for the generalized non-linear Schrödinger system, *J. Comput. Math.* 1 (1983) 116–129.